

DTIC FILE COPY

2

# NAVAL POSTGRADUATE SCHOOL

## Monterey, California

AD-A228 058



DTIC  
ELECTE  
OCT 24 1990  
S B D  
Co

### THESIS

MEASUREMENT OF THE CAPTURE EFFECT OF  
FREQUENCY MODULATION

by

Dennis G. Bevington

December 1989

Thesis Advisor

G. A. Myers

Approved for public release; distribution is unlimited.

90 10 28 117

Unclassified

security classification of this page

## REPORT DOCUMENTATION PAGE

1a Report Security Classification <b>Unclassified</b>			1b Restrictive Markings		
2a Security Classification Authority			3 Distribution/Availability of Report		
2b Declassification/Downgrading Schedule			<b>Approved for public release; distribution is unlimited.</b>		
4 Performing Organization Report Number(s)			5 Monitoring Organization Report Number(s)		
6a Name of Performing Organization <b>Naval Postgraduate School</b>		6b Office Symbol (if applicable) <b>32</b>	7a Name of Monitoring Organization <b>Naval Postgraduate School</b>		
6c Address (city, state, and ZIP code) <b>Monterey, CA 93943-5000</b>			7b Address (city, state, and ZIP code) <b>Monterey, CA 93943-5000</b>		
8a Name of Funding Sponsoring Organization		8b Office Symbol (if applicable)	9 Procurement Instrument Identification Number		
8c Address (city, state, and ZIP code)			10 Source of Funding Numbers		
			Program Element No	Project No	Task No
			Work Unit Accession No		
11 Title (include security classification) <b>MEASUREMENT OF THE CAPTURE EFFECT OF FREQUENCY MODULATION</b>					
12 Personal Author(s) <b>Dennis G. Bevington</b>					
13a Type of Report <b>Master's Thesis</b>		13b Time Covered From To		14 Date of Report (year, month, day) <b>December 1989</b>	
				15 Page Count <b>76</b>	
16 Supplementary Notation <b>The views expressed in this thesis are those of the author and do not reflect the official policy or position of the Department of Defense or the U.S. Government.</b>					
17 Cosati Codes			18 Subject Terms (continue on reverse if necessary and identify by block number)		
Field	Group	Subgroup	Capture Effect, FM, demodulation.		
19 Abstract (continue on reverse if necessary and identify by block number)					
<p>Capture Effect is a phenomenon associated with frequency modulation (FM). The capture effect relates the ability of the receiver demodulator to recover the message of the dominant carrier when two or more FM carriers of unequal power level are present. In this research, an experimental system is constructed that generates the sum of two FM signals and demodulates that sum using a phase-locked loop (PLL). The effect on capture by several parameters is measured. These parameters are the frequency deviation of the FM signal, the frequency of the message, and the lowpass filter design of the PLL demodulator. Capture ratios as small as 0.387 dB are observed. Results show that the frequency deviation of the stronger signal affects capture. The frequency deviation of the weaker signal has no effect on capture. Frequencies of the messages have small effects on capture.</p> <p>(H) →</p>					
20 Distribution Availability of Abstract			21 Abstract Security Classification		
<input checked="" type="checkbox"/> unclassified unlimited <input type="checkbox"/> same as report <input type="checkbox"/> DTIC users			<b>Unclassified</b>		
22a Name of Responsible Individual <b>G. A. Myers</b>			22b Telephone (include Area code) <b>(408) 646-2325</b>		22c Office Symbol <b>62Mv</b>

DD FORM 1473, 84 MAR

83 APR edition may be used until exhausted  
All other editions are obsolete

security classification of this page

Unclassified

Approved for public release; distribution is unlimited.

Measurement of the Capture Effect of  
Frequency Modulation

by

Dennis G. Bevington  
Lieutenant, United States Navy  
B.S., United States Naval Academy, 1983

Submitted in partial fulfillment of the  
requirements for the degree of

MASTER OF SCIENCE IN ELECTRICAL ENGINEERING

from the

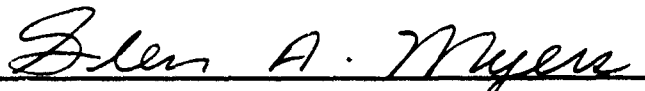
NAVAL POSTGRADUATE SCHOOL  
December 1989

Author:



Dennis G. Bevington

Approved by:



G. A. Myers, Thesis Advisor



T.T. Ha, Second Reader



John P. Powers, Chairman,  
Department of Electrical Engineering

## ABSTRACT.

Capture Effect is a phenomenon associated with frequency modulation (FM). The capture effect relates the ability of the receiver demodulator to recover the message of the dominant carrier when two or more FM carriers of unequal power level are present. In this research, an experimental system is constructed that generates the sum of two FM signals and demodulates that sum using a phase-locked loop (PLL). The effect on capture by several parameters is measured. These parameters are the frequency deviation of the FM signal, the frequency of the message, and the lowpass filter design of the PLL demodulator.

Capture ratios as small as 0.387 dB are observed. Results show that the frequency deviation of the stronger signal affects capture. The frequency deviation of the weaker signal has no effect on capture. Frequencies of the messages have small effects on capture.

Accession For	
NTIS GRA&I	<input checked="checked" type="checkbox"/>
DTIC TAB	<input type="checkbox"/>
Unannounced	<input type="checkbox"/>
Justification	
By	
Distribution/	
Availability Codes	
Dist	Avail and/or Special
A-1	



## TABLE OF CONTENTS

I. INTRODUCTION .....	1
II. BACKGROUND .....	2
A. EQUATION FOR AN FM CARRIER. ....	2
B. CAPTURE EFFECT .....	2
C. ANALYSIS .....	3
III. EXPERIMENTAL SYSTEM .....	6
A. SYSTEM COMPONENTS .....	6
1. Transmitter .....	6
2. Receiver .....	12
B. EXPERIMENTAL PROCEDURES .....	14
1. Parameters Measured .....	16
2. Message Types .....	17
IV. EXPERIMENTAL RESULTS .....	18
A. SIGNAL BANDWIDTH .....	18
B. SIGNAL FREQUENCY .....	33
C. PLL FILTER BANDWIDTH AND DESIGN .....	42
V. CONCLUSIONS .....	53
APPENDIX A. CIRCUIT SCHEMATICS .....	54
A. TRANSMITTER. ....	54
B. RECEIVER. ....	56
APPENDIX B. PLL LOWPASS FILTER DESIGN. ....	59
LIST OF REFERENCES .....	64
INITIAL DISTRIBUTION LIST .....	65

## LIST OF FIGURES

Figure 1.	Photograph of Test Bench and Associated Equipment. ....	7
Figure 2.	Block Diagram of the Transmitter. ....	8
Figure 3.	VCO Characteristics. ....	9
Figure 4.	VCO Output for Square Wave Inputs for Frequency Deviation of 2.5 kHz (top trace) and 5.0 kHz (bottom trace). ....	10
Figure 5.	VCO Output for Square Wave Inputs for Frequency Deviation of 7.5 kHz (top trace) and 10.0 kHz (bottom trace). ....	11
Figure 6.	Block Diagram of the Receiver. ....	13
Figure 7.	PLL Loop Filter Design. ....	15
Figure 8.	Demodulator Output (upper trace) and Message (lower trace) for Frequency Deviation of 1 kHz. ....	19
Figure 9.	Demodulator Output (upper trace) and Message (lower trace) for Frequency Deviation of 1.25 kHz. ....	20
Figure 10.	Demodulator Output (upper trace) and Message (lower trace) for Frequency Deviation of 2.0 kHz. ....	21
Figure 11.	Demodulator Output (upper trace) and Message (lower trace) for Frequency Deviation of 2.5 kHz. ....	22
Figure 12.	Demodulator Output (upper trace) and Message (lower trace) for Frequency Deviation of 3.75 kHz. ....	23
Figure 13.	Demodulator Output (upper trace) and Message (lower trace) for Frequency Deviation of 5.0 kHz. ....	24
Figure 14.	Demodulator Output (upper trace) and Message (lower trace) for Frequency Deviation of 6.25 kHz. ....	25
Figure 15.	Demodulator Output (upper trace) and Message (lower trace) for Frequency Deviation of 7.5 kHz. ....	26
Figure 16.	Demodulator Output (upper trace) and Message (lower trace) for Frequency Deviation of 8.75 kHz. ....	27
Figure 17.	Demodulator Output (upper trace) and Message (lower trace) for Frequency Deviation of 10.0 kHz. ....	28
Figure 18.	Capture Ratio vs. Frequency Deviation of Carriers A and B. ....	29
Figure 19.	Capture Ratio vs. Frequency Deviation of Carrier A when the Frequency	

Deviation of Carrier B is 2.5 kHz. ....	30
Figure 20. Capture Ratio vs. Frequency Deviation of Carrier A when the Frequency Deviation of Carrier B is 6.25 kHz. ....	31
Figure 21. Capture Ratio vs. Frequency Deviation of Carrier A when the Frequency Deviation of Carrier B is 10.0 kHz. ....	32
Figure 22. Capture Ratio (A/B) vs. Frequency Deviation of Carrier A where the Frequency Deviation of B is 2.5, 6.25 and 10.0 kHz. ....	34
Figure 23. Demodulator Output (upper trace) and Message (lower trace) for Fre- quency Deviation of 3 kHz. ....	35
Figure 24. Demodulator Output (upper trace) and Message (lower trace) for Fre- quency Deviation of 5.5 kHz. ....	36
Figure 25. Demodulator Output (upper trace) and Message (lower trace) for Fre- quency Deviation of 7 kHz. ....	37
Figure 26. Capture Ratio vs. Frequency Deviation of Carriers A and B. ....	38
Figure 27. Capture Ratio vs. Frequency Deviation of Carrier A when the Frequency Deviation of B is 2.5 kHz. ....	39
Figure 28. Capture Ratio vs. Frequency Deviation of Carrier A when the Frequency Deviation of B is 6.25 kHz. ....	40
Figure 29. Capture Ratio vs. Frequency Deviation of Carrier A when the Frequency Deviation of B is 10.0 kHz. ....	41
Figure 30. Capture Ratio (A/B) vs. Frequency Deviation of Carrier A when the Frequency Deviation of B is 2.5 kHz. ....	43
Figure 31. Capture Ratio (A/B) vs. Frequency Deviation of Carrier A when the Frequency Deviation of B is 6.25 kHz. ....	44
Figure 32. Capture Ratio (A/B) vs. Frequency Deviation of Carrier A when the Frequency Deviation of B is 10.0 kHz. ....	45
Figure 33. PLL Loop Filter Output (lower trace) and Post Detection Filter Output (upper trace) for Sine Wave Message. ....	46
Figure 34. PLL Loop Filter Output (lower trace) and Post Detection Filter Output (upper trace) for Square Wave Message. ....	47
Figure 35. Capture Ratio (A/B) vs. Bandwidth of PLL Loop Filter. ....	49
Figure 36. Capture Ratio (B/A) vs. Bandwidth of PLL Loop Filter. ....	50
Figure 37. Capture Ratio (A/B) vs. Bandwidth of PLL Loop Filter. ....	51
Figure 38. Capture Ratio (A/B) vs. Bandwidth of PLL Loop Filter. ....	52
Figure 39. Schematic Diagram of the Transmitter. ....	55

Figure 40. Schematic Diagram of the Receiver. ....	57
Figure 41. PLL Filter Designs. ....	60
Figure 42. Frequency Response of the PLL Loop Filters. ....	63



## LIST OF SYMBOLS AND ABBREVIATIONS

<b>A</b>	Designates the 'A' Side of the Transmitter
<b>A/B</b>	Capture Ratio in decibels when Message A is Dominant
<b><math>A_c</math></b>	Peak Amplitude of Carrier
<b><math>A_1</math></b>	Peak Amplitude of Carrier 1
<b><math>A_2</math></b>	Peak Amplitude of Carrier 2
<b>B</b>	Designates the 'B' Side of the Transmitter
<b>B/A</b>	Capture Ratio in decibels when Message B is Dominant
<b>b</b>	Bandwidth of the Message
<b>BW</b>	Bandwidth of an FM Signal
<b>C</b>	Peak Amplitude of Carrier 3
<b><math>C_x</math></b>	Capacitor 'x'
<b><math>\delta</math></b>	Damping Ratio
<b><math>\epsilon</math></b>	Carrier Offset
<b><math>f_A</math></b>	Frequency of Message A
<b><math>f_B</math></b>	Frequency of Message B
<b><math>f_{BW}</math></b>	Corner Frequency of Postprocessing Filter
<b><math>f_c</math></b>	Carrier Frequency
<b><math>f_{CAP}</math></b>	Capture Range of Phase-Locked Loop
<b><math>f_i(t)</math></b>	Instantaneous Frequency
<b><math>f_L</math></b>	Lock Range of Phase-Locked Loop
<b><math>f_n</math></b>	Corner Frequency of PLL Loop Filter
<b><math>f_o</math></b>	Phase-Locked Loop Rest Frequency
<b><math>f_{oc}</math></b>	Phase-Locked Loop Center Frequency
<b><math>\Delta f</math></b>	Frequency Deviation of Carrier
<b><math>\Delta f_i(t)</math></b>	Change in Instantaneous Frequency
<b>FM</b>	Frequency Modulation
<b><math>f_R</math></b>	VCO Rest Frequency
<b>Hz</b>	Hertz
<b>IC</b>	Integrated Circuit
<b><math>k_f</math></b>	Constant Having Units of Hertz per Volt
<b><math>k_n</math></b>	Constant (Hertz per Volt) for Modulator 1

$k_f$	Constant (Hertz per Volt) for Modulator 2
$K_o K_d$	Internal Gains of PLL
$m(t)$	Baseband Message Voltage
$m_1(t)$	Baseband Message 1
$m_2(t)$	Baseband Message 2
$M_p$	Peak Amplitude of the Message
op amp	Operational Amplifier
$\Omega$	Ohm
$P_A$	Power of Signal A
$P_B$	Power of Signal B
PLL	Phase-Locked Loop
$\phi_1(t)$	Argument of Angle-Modulated Sinusoid 1
$\phi_2(t)$	Argument of Angle-Modulated Sinusoid 2
$\phi_3(t)$	Argument of Angle-Modulated Sinusoid 3
$\phi_i(t)$	Argument of Angle-Modulated Sinusoid
$r$	Capture Ratio
$r_{dB}$	Capture Ratio in decibels
RMS	Root Mean Squared
$R_x$	Resistor 'x'
$s(t)$	Equation for Angle-Modulated Sinusoid
$s_1(t)$	Sinusoidal Carrier for Message 1
$s_2(t)$	Sinusoidal Carrier for Message 2
$\tau_1$	Time Constant 1
$\tau_2$	Time Constant 2
$V$	RMS Voltage of Carrier
$V_A$	RMS Voltage of Carrier A
$V_B$	RMS Voltage of Carrier B
$V_{Ap}$	Peak Voltage of Carrier A
$V_{Bp}$	Peak Voltage of Carrier B
$V_{cc}$	Supply Voltage
$v(t)$	Sum of FM Signals 1 and 2
VCO	Voltage-Controlled Oscillator
$V_p$	Peak Voltage of Carrier

## I. INTRODUCTION

Frequency modulation (FM) occurs when the frequency of a sinusoidal carrier is caused to vary in accordance with the voltage of the message to be carried (transmitted). An advantage of FM is that it provides increased discrimination against noise. The disadvantage of FM that accompanies the increased performance in noise is that the required bandwidth for FM signals is also increased [Ref. 1: p. 180].

A phenomenon associated with FM is capture effect. The capture effect relates the ability of the demodulator to recover the message of the dominant carrier when two or more FM carriers are present. This research deals exclusively with this phenomenon and experimentally investigates its characteristics.

Although computer simulation of capture effect can be done and is very useful in verifying the origin of the capture effect of FM demodulators, an improved understanding results from operation of an experimental system where parameters can be varied at will with real-time measurements and observations made [Ref. 2]. The experimental system consists of a transmitter that creates the sum of two FM signals and sends this sum to a receiver that demodulates the composite signal. When capture occurs, the receiver output is the message of the dominant carrier.

Chapter II presents background information on FM and capture effect. Chapter III is a description of the experimental system and of how measurements are made in determining capture ratio, a parameter of capture effect. Chapter IV contains the actual experimental results. Conclusions are listed in Chapter V. Detailed schematics of the experimental system are given in Appendix A. Appendix B is a detailed description of the phase-locked loop (PLL) lowpass filter design. The PLL is used as the demodulator for the FM signals generated in this research and the filter design is one of the parameters that is investigated. A list of references is provided.

## II. BACKGROUND

### A. EQUATION FOR AN FM CARRIER.

The general equation for an angle modulated sinusoid is

$$s(t) = A_c \cos[\phi_f(t)] \quad (2.1)$$

where  $A_c$  is the peak amplitude of the carrier. The sinusoid completes one period (cycle) when  $\phi_f(t)$  changes by  $2\pi$  radians. The instantaneous frequency  $f_f(t)$  is defined as

$$f_f(t) = \left( \frac{1}{2\pi} \right) \frac{d\phi_f(t)}{dt} \quad (2.2)$$

If  $f_f(t)$  varies in accordance with a message or baseband voltage  $m(t)$ , then we have frequency modulation (FM). The instantaneous frequency for FM is typically defined to be

$$f_f(t) = f_c + k_f m(t) \quad (2.3)$$

where  $f_c$  is the carrier frequency and  $k_f$  is a constant having units of Hertz per volt. The constant  $k_f$  is a characteristic of the modulator. By combining equations (2.2) and (2.3), an expression for  $\phi_f(t)$  that includes the message voltage is

$$\phi_f(t) = 2\pi f_c t + 2\pi k_f \int_0^t m(\tau) d\tau \quad (2.4)$$

In the above equation, the angle of the unmodulated carrier is assumed to be zero at  $t=0$ . Combining equation (2.4) with equation (2.1) gives the expression for the frequency modulated carrier as

$$s(t) = A_c \cos[2\pi f_c t + 2\pi k_f \int_0^t m(\tau) d\tau] \quad (2.5)$$

### B. CAPTURE EFFECT

When more than one frequency modulated signal is applied to a demodulator and these two signals are in the same frequency band, the phenomenon of capture effect

occurs. The result of capture can be explained as follows. Let  $s(t)$  equal the sum of two unrelated sinusoidal carriers modulated by different messages  $m_1(t)$  and  $m_2(t)$ . In equation form this means

$$s(t) = s_1(t) + s_2(t) \quad (2.6)$$

where

$$\begin{aligned} s_1(t) &= A_1 \cos[2\pi f_c t + 2\pi k_{f1} \int_0^t m_1(\tau) d(\tau)] \\ s_2(t) &= A_2 \cos[2\pi(f_c + \varepsilon)t + 2\pi k_{f2} \int_0^t m_2(\tau) d(\tau)] \end{aligned} \quad (2.7)$$

When  $s(t)$  is present at the input of the demodulator and if  $A_1 > A_2$ , then  $m_1(t)$  appears at the output of the demodulator. Likewise, if  $A_2 > A_1$ , then  $m_2(t)$  appears at the output of the demodulator. The constants  $k_{f1}$  and  $k_{f2}$  are associated with the two separate modulators. The carrier offset  $\varepsilon$  is any value such that  $s_1(t)$  and  $s_2(t)$  are in the same operating frequency band of the receiver demodulator. When capture occurs, there is no evidence of the existence of the message of the weaker carrier at the demodulator output. This phenomenon is known as capture effect. The demodulator of interest in this research is the phase-locked loop (PLL).

### C. ANALYSIS

In an attempt to mathematically explain capture effect, it is necessary to obtain an expression for the instantaneous frequency of the sum of two frequency-modulated signals. This is done because the output of a frequency demodulator such as the PLL is proportional to  $f(t) - f_c \equiv \Delta f(t)$  [Ref. 3]. To obtain  $f(t)$  for the sum of two frequency-modulated carriers, it is practical to start with

$$v(t) = A_1 \cos \phi_1(t) + A_2 \cos \phi_2(t) \quad (2.8)$$

where  $v(t)$  is the sum of the two signals. Using trigonometric identities, Eq(2.8) can be written as

$$v(t) = C \cos \phi_3(t) \quad (2.9)$$

where

$$C^2 = A_1^2 + A_2^2 + 2A_1A_2 \cos[\phi_1(t) - \phi_2(t)] \quad (2.10)$$

and

$$\tan \phi_3(t) = \frac{(A_1 \sin \phi_1(t) + A_2 \sin \phi_2(t))}{(A_1 \cos \phi_1(t) + A_2 \cos \phi_2(t))} \quad (2.11)$$

From the original equation for instantaneous frequency given in (2.2), then

$$\begin{aligned} f_i(t) &= \left( \frac{1}{2\pi} \right) \left[ \frac{d\phi_3(t)}{dt} \right] \\ &= \left( \frac{1}{2\pi} \right) \frac{d}{dt} \tan^{-1} \left[ \frac{(A_1 \sin \phi_1(t) + A_2 \sin \phi_2(t))}{(A_1 \cos \phi_1(t) + A_2 \cos \phi_2(t))} \right] + f_c \\ &= \frac{A_1^2 \frac{d\phi_1}{dt} + A_2^2 \frac{d\phi_2}{dt} + [A_1A_2 \cos(\phi_1 - \phi_2)] \left( \frac{d\phi_1}{dt} + \frac{d\phi_2}{dt} \right)}{2\pi[A_1^2 + A_2^2 + 2A_1A_2 \cos(\phi_1 - \phi_2)]} + f_c \end{aligned} \quad (2.12)$$

Note that  $\phi_1$  and  $\phi_2$  are given by equation (2.4) and

$$\frac{d\phi_j}{dt} = 2\pi f_c + 2\pi k_{fj} m_j(t) \quad j = 1, 2. \quad (2.13)$$

Subtracting  $f_c$  from (2.12) will give  $\Delta f(t)$ . It can be seen that this is a difficult equation to analyze and is not useful in predicting the behavior of a demodulator. It is equally difficult to use this equation to explain capture effect.

Computer simulations of the instantaneous frequency equations have been done when the messages  $m_1(t)$  and  $m_2(t)$  are assumed to be sinusoids of different frequencies and the two signals  $s_1(t)$  and  $s_2(t)$  have the same carrier frequencies. The results of that research indicate that the lowpass filter in the demodulator accounts for the capture effect of FM receivers. The effect of averaging by the lowpass filter creates capture. Simulation indicates capture can occur when the value of capture ratio is as small as 0.17 dB. (Capture ratio is defined as the ratio of the amplitude of the two frequency modulated carriers [Ref. 2: p. 18].)

Analysis has also been done which results in a simplified formula for evaluating capture ratio in frequency modulation. That analysis concentrated on the effects of the demodulator bandwidth. It also includes several simplifying approximations that are not strictly justified throughout an entire period of a periodic message signal [Ref. 4: p. 783].

Experimental verification of capture effect can explore many parameters and properties of the phenomenon of capture effect that are not readily apparent from mathematical formulas or easily simulated by computer. An experimental system is not limited to the simple sinusoids that are used in computer simulations. Also, parameters are easily changed and monitored, and results are quickly obtained.

In this research, a transmitter and receiver are designed, built, tested and operated. Capture effect is observed and capture ratio is measured as a function of system parameters of interest.

### III. EXPERIMENTAL SYSTEM

The system built to measure the capture effect of frequency demodulators consists of a transmitter and a receiver. Two FM carriers are generated and summed in the transmitter. This composite voltage is then passed to the receiver on a piece of wire. The receiver consists of a single demodulator. The system uses standard integrated circuit chips and various pieces of test equipment. Figure 1 on page 7 is a photograph of the test bench and associated circuitry and equipment. A detailed description of the test circuitry is contained in Appendix A.

#### A. SYSTEM COMPONENTS

##### 1. Transmitter

To measure capture effect, two frequency modulated signals must be present at the input to the receiver demodulator. To accurately control and measure the parameters of both signals, two separate transmitters were constructed. Figure 2 on page 8 shows a block diagram of the transmitter that was built. The two separate channels are labeled A and B. Both channels are identical, so a description of channel A is sufficient.

The message is generated using a standard Wavetek signal generator. The messages are periodic sine waves, square waves or triangle waves. The input message source has a gain adjustment which controls the peak frequency deviation of the FM carrier.

An LM8038 voltage-controlled oscillator (VCO) integrated circuit (IC) is used as a modulator. Figure 3 on page 9 is a plot of the output frequency of the VCO vs. input voltage for both channels A and B. The region about 65 kHz is more linear than others. Therefore, the VCO is designed to have a rest frequency of 64.5 kHz. Typical VCO output waveforms for a sine wave input and a square wave input are shown in Figure 2. A further demonstration of the operation of the VCO is shown by Figure 4 on page 10 and Figure 5 on page 11 where the modulating voltage is a square wave of four different amplitudes.

The amplitude of the output of each VCO is controlled with another gain adjustment. It is here that the level of each of the frequency modulated signals can be accurately adjusted and measured.

A summing amplifier combines the two frequency modulated signals which are then sent to the receiver. A photograph of the output of the summing amplifier is given





**Figure 1. Photograph of Test Bench and Associated Equipment.**

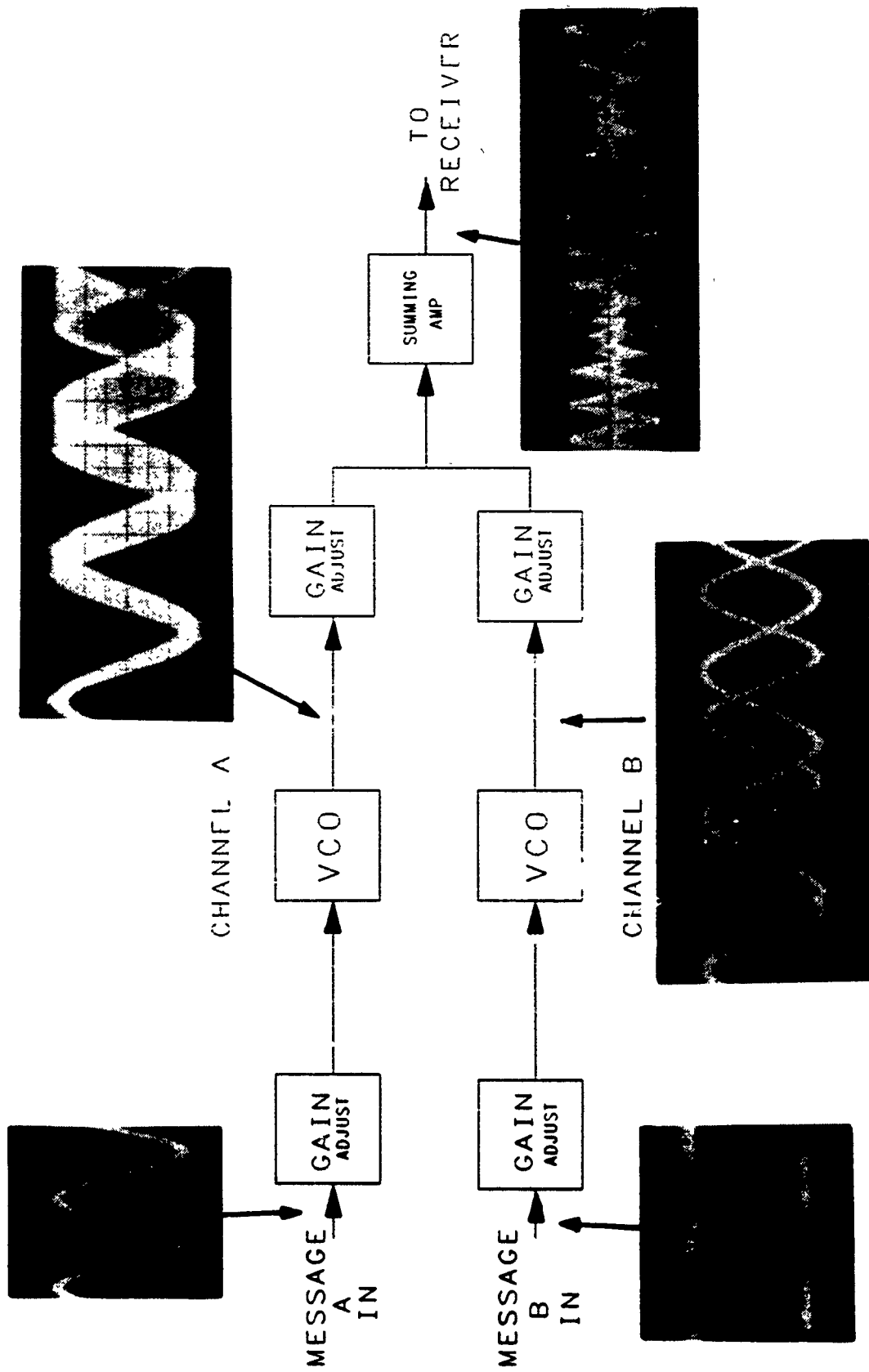


FIG. 2 BLOCK DIAGRAM OF THE TRANSMITTER.

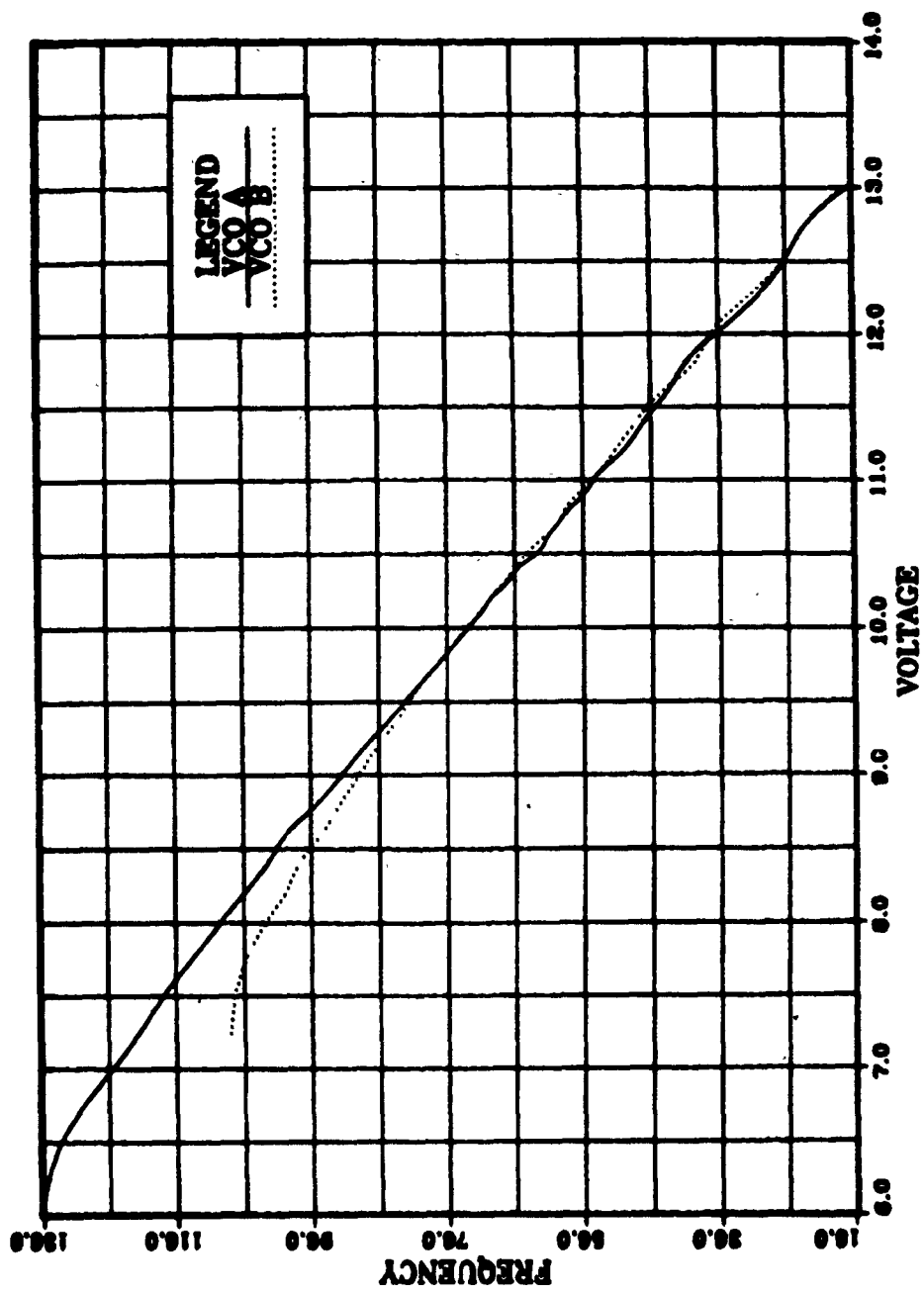
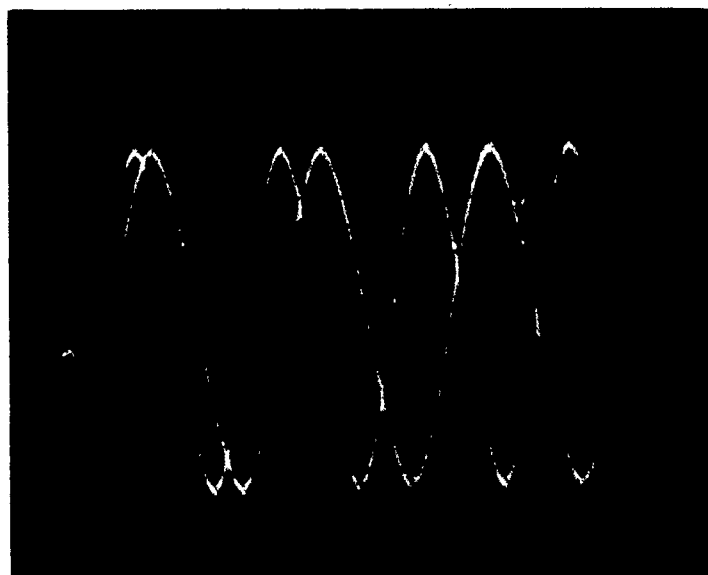
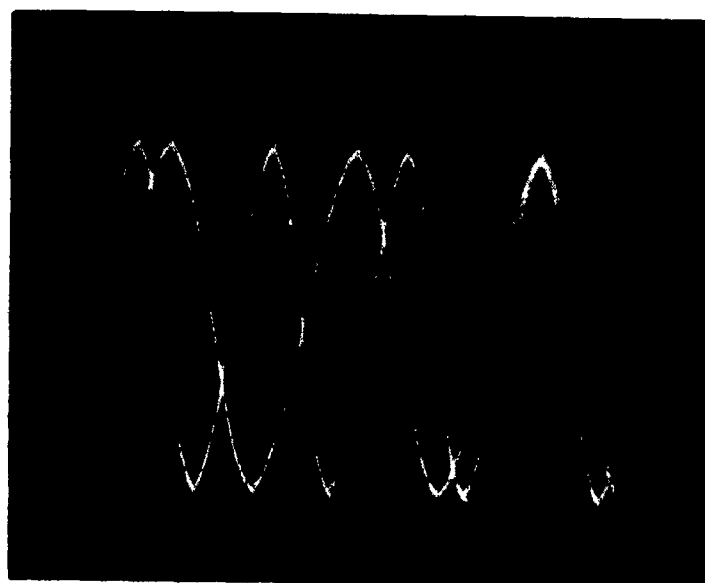
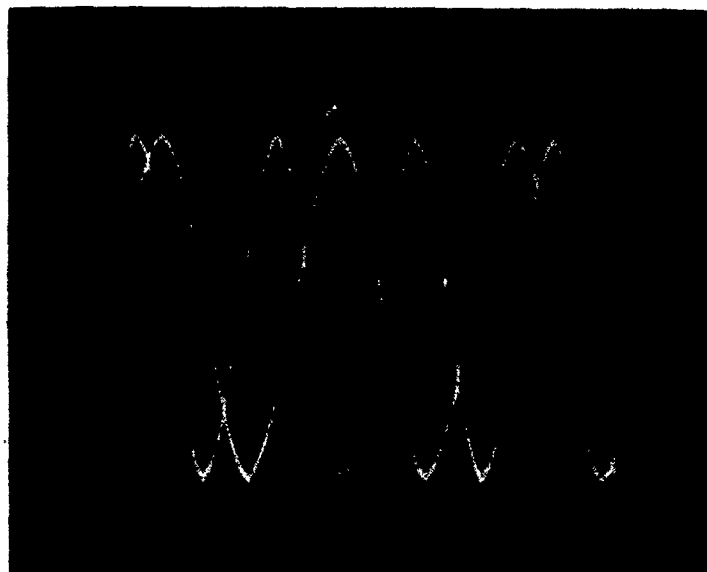


Figure 3. VCO Characteristics.



**Figure 4. VCO Output for Square Wave Inputs for Frequency Deviation of 2.5 kHz (top trace) and 5.0 kHz (bottom trace).**



**Figure 5. VCO Output for Square Wave Inputs for Frequency Deviation of 7.5 kHz (top trace) and 10.0 kHz (bottom trace).**

in Figure 2 for the case of a carrier frequency modulated by a square wave being added with a carrier frequency modulated by a sine wave.

## 2. Receiver

The receiver is designed not only to demodulate a frequency modulated signal but also to accurately observe the phenomenon of capture. Figure 6 on page 13 is a block diagram of the receiver that was built.

The signal from the transmitter is applied to a hard limiter in order to preserve the zero crossings of the sum of signals A and B, to eliminate any amplitude modulation that is present on the signal and to accommodate the PLL used as a demodulator. The voltage follower immediately preceding the hard limiter is there solely for impedance matching of the summer in the transmitter to the hard limiter.

A photograph of the output of the hard limiter is shown in Figure 6. This is the output of the summing amplifier in Figure 2 after it has passed through the voltage follower and the hard limiter.

After hard limiting, the signal is applied directly to the PLL. The PLL demodulates the input signal. It is here in the frequency demodulator where capture occurs. Figure 6 shows the output of the PLL for the case of the dominant carrier modulated by a sinusoid.

As discussed later in this chapter and in Appendix B, the lowpass filter of the PLL is designed to optimize both the capture effect measurements and signal clarity. It turns out that these two parameters are somewhat opposed and a compromise must be made. Thus, there is a need for a post-processing filter to eliminate some of the higher frequency noise from the PLL output. This is common practice in use of a PLL as a demodulator.

Two active lowpass filters are constructed with 1 kHz and 3 kHz bandwidths. These filters are effective as post-detection filters, and they permit improved observation of capture effect. Figure 6 is a photograph of the output of the active filter when the modulation on the dominant carrier is a sinusoid.

The photographs in Figure 6 correspond to those of the transmitter voltages in Figure 2. It can be seen in Figure 2 that the peak amplitude of the frequency modulated signal of channel A is slightly larger than that of channel B. The captured signal modulation is shown in Figure 6, and it is the sinusoid that modulated the carrier of channel A. Note that there is no trace of the modulation on the carrier of channel B in the output of the receiver. These results are documented in chapters IV and V.

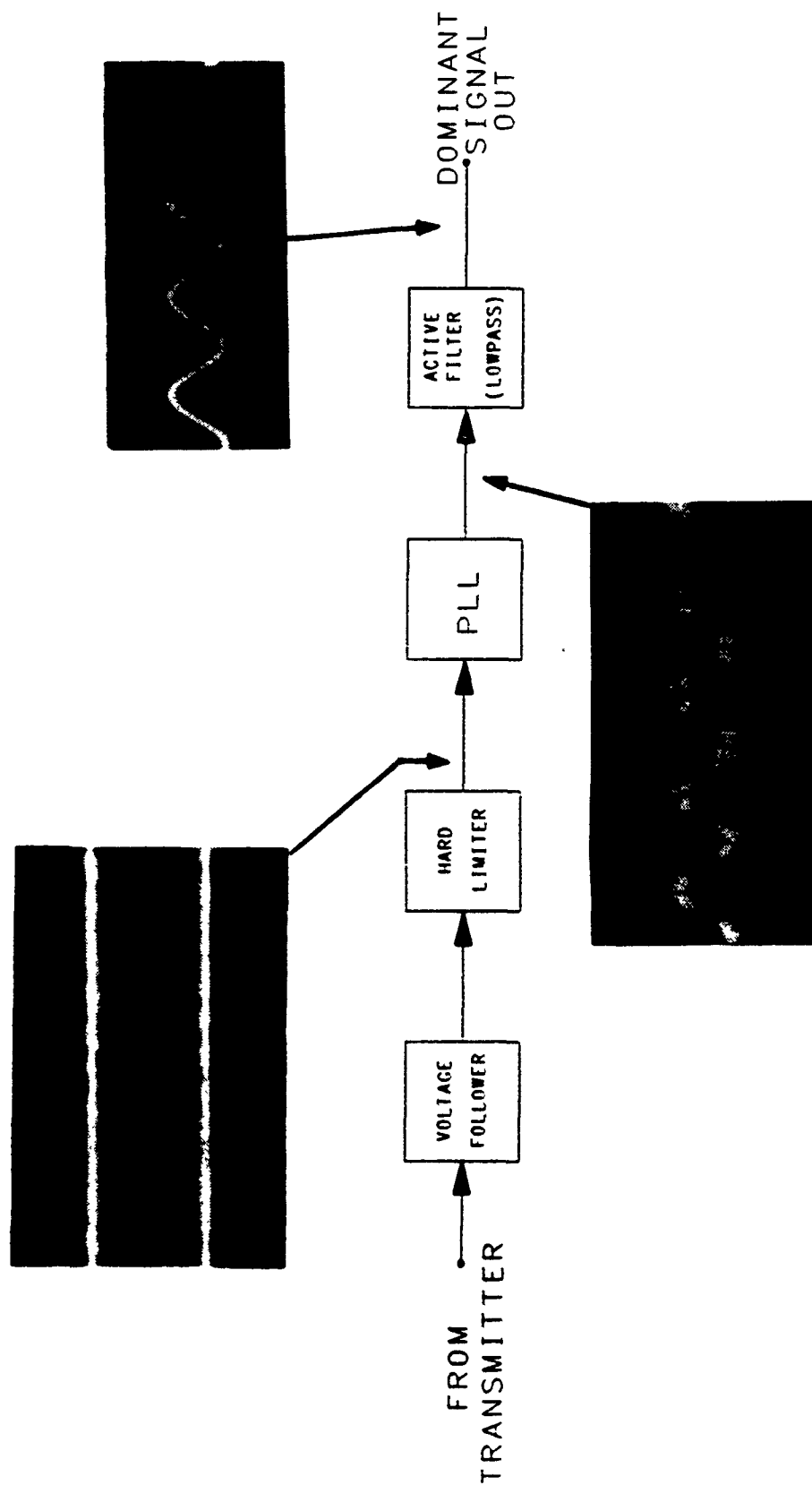


FIG. 6 BLOCK DIAGRAM OF THE RECEIVER.

The integrated circuit that was chosen for the PLL allowed two basic designs for the loop lowpass filter. These two designs are the simple RC lowpass filter and the lag-lead lowpass filter. Figure 7 on page 15 is an illustration of these two filters and their location inside of the PLL curcuitry. A detailed description of their design is given in Appendix B. A comparison is made between the performance of these two designs based on their bandwidth and their contribution to capture effect.

## B. EXPERIMENTAL PROCEDURES

Emphasis is placed on measuring the capture ratio of the frequency modulated signals and the effect of various parameters on capture. Capture ratio  $r$  is defined as the power of the dominant signal divided by the power of the weaker signal. That is,

$$r = \frac{P_A}{P_B} \quad (3.1)$$

where  $P_A$  is the power of signal A and  $P_B$  is the power of signal B. By observing the frequency modulated signals on a dual-trace ocsilloscope, the peak voltage of each signal can be observed. The ratio of peak voltages also determines capture ratio because

$$\frac{P_A}{P_B} = \frac{\left( \frac{(V_{Ap})^2}{2} \right)}{\left( \frac{(V_{Bp})^2}{2} \right)} = \frac{(V_{Ap})^2}{(V_{Bp})^2} \quad (3.2)$$

where  $V_{Ap}$  is the peak voltage of signal A and  $V_{Bp}$  is the peak voltage of signal B.

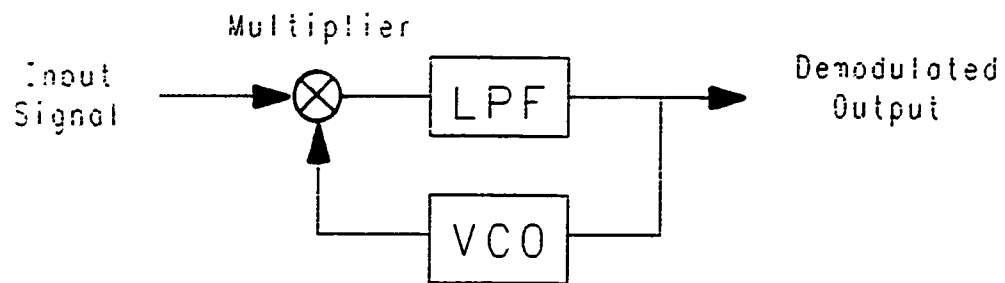
The root mean squared (RMS) voltage of each signal is also obtained using an RMS voltmeter. Since the carrier frequency is a sinusoid, the relationship between RMS and peak voltage  $V_p$  is

$$V = \frac{V_p}{\sqrt{2}} \quad (3.3)$$

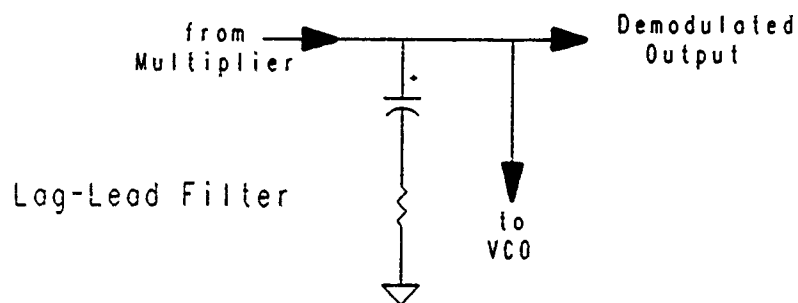
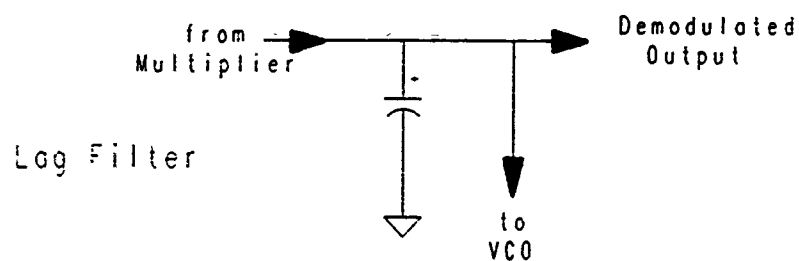
Therefore, in terms of RMS voltages, capture ratio is

$$r = \frac{V_A^2}{V_B^2} \quad (3.4)$$





(a) Phase Locked Loop Block Diagram.



(b) Lowpass Filter Design Choices.

**Figure 7. PLL Loop Filter Design.**

where  $V_A$  is the RMS voltage of signal A and  $V_B$  is the RMS voltage of signal B. The relationship using RMS voltages is preferred since the RMS voltages from the RMS voltmeter are more accurately measured than peak voltages obtained from the oscilloscope. In decibels, the capture ratio  $r_{dB} = 10 \log(r)$ .

To determine that a signal is captured, the output of the post processing filter is monitored using an oscilloscope. The amplitude of the frequency modulated signal of one channel is varied while the amplitude of the other channel is held constant. When both carriers are at the same amplitude level, the output is random appearing (noise-like). As the level of one signal is increased, the oscilloscope trace becomes regular. When the signal appearing on the oscilloscope has no apparent effect caused by the suppressed signal, the RMS voltage levels out of the VCO are measured and capture ratio is determined. It should be noted that the determination of when capture occurs is subjective.

### 1. Parameters Measured

It is known that the FM signal of larger amplitude value will capture a weaker FM signal. This research considered other signal parameters and their effect on capture.

The effect of signal bandwidth on capture was studied. Signal bandwidth (BW) for an FM signal is approximated by Carson's Rule which is

$$BW = 2(b + \Delta f) \quad (3.5)$$

where  $\Delta f$  is the peak frequency deviation of the carrier frequency and  $b$  is the bandwidth of the message. The frequency deviation  $\Delta f$  is determined by the amplitude of the message from the signal generators. The frequency deviation  $\Delta f$  can thus be accurately measured by measuring the peak voltage of the message  $M_p$ , and then determining the frequency deviation from the VCO frequency-voltage characteristics given in Figure 3. From this figure it is ascertained that the slope of the curve in the region of operation is 17.9 kHz/Volt. Therefore,

$$\Delta f = M_p(17.9) \quad \text{in kHz} \quad (3.6)$$

From Carson's Rule, when the message bandwidth is held constant, the bandwidth of the FM carrier is proportional to  $\Delta f$ . The parameter  $\Delta f$  is measured and plotted to determine the effect of bandwidth on capture ratio. The value of  $\Delta f$  is varied from 1 kHz to 12 kHz, where the lower limit is based on the signal being above the noise level of the

PLL, and where the upper limit is based on the capture range of the PLL and the linearity of the VCO.

From Carson's Rule, message bandwidth  $b$  is simply the frequency of the input message when the message is a single sinusoid. Thus, the frequency of the input message is also measured to determine its effect on capture. The frequency of the input message ranges from 75 Hz to 400 Hz. These low frequencies are chosen based on the ability to demodulate a message using a 3 kHz lowpass filter in the demodulator. A square wave message at 400 Hz will show no distortion at the output of the post-processing filter since its first three harmonics will not be attenuated by the 3 kHz lowpass filter. Three kilohertz is also a typical bandwidth of voice messages.

The final parameter that is analysed is the bandwidth and design of the loop filter in the PLL. The bandwidth of this filter is determined using equations given in Appendix B. The two designs that are chosen are the simple lag filter and the lag-lead filter. Bandwidth values range from 3 kHz to infinity.

## **2. Message Types**

The three message types are sinusoid, square wave and triangular wave. In almost all of the cases, the square wave is used as a message to determine the upper bound of the capture ratio. This is based on the fact that the square wave has the largest bandwidth and will be the most limiting of the three message types.

After observing capture on the oscilloscope using the square wave, the dominant signal message is changed to a sinusoid and then to a triangle wave to verify capture. Then, the suppressed signal message is changed to a sinusoid and to a triangular wave to ensure the demodulator output is not affected.

## IV. EXPERIMENTAL RESULTS

Extensive measurements made on system operation include various combinations of parameters. The parameters are the bandwidth of each carrier, the frequency of the messages and the PLL filter bandwidth and design. These parameters are all varied to determine their effect on the capture ratio of the two frequency modulated carriers.

The result of interest is the ratio of amplitudes of the frequency modulated signals. Capture ratios as small as 0.382 dB were measured.

### A. SIGNAL BANDWIDTH

The first set of data is taken for message frequencies of 100 Hz for channel A and 75 Hz for channel B. From Carson's Rule, when the message frequency is held constant, signal bandwidth will be proportional to the peak frequency deviation  $\Delta f$  of the carrier. Therefore, the term  $\Delta f$  is linearly related to bandwidth. Here,  $\Delta f$  is varied from 1 kHz to 12 kHz. Figures 8 through 17 are photographs of the dominant signal message at the demodulator postprocessing filter output. By viewing these pictures for various  $\Delta f$ , the signal shape and clarity where capture occurs can be observed.

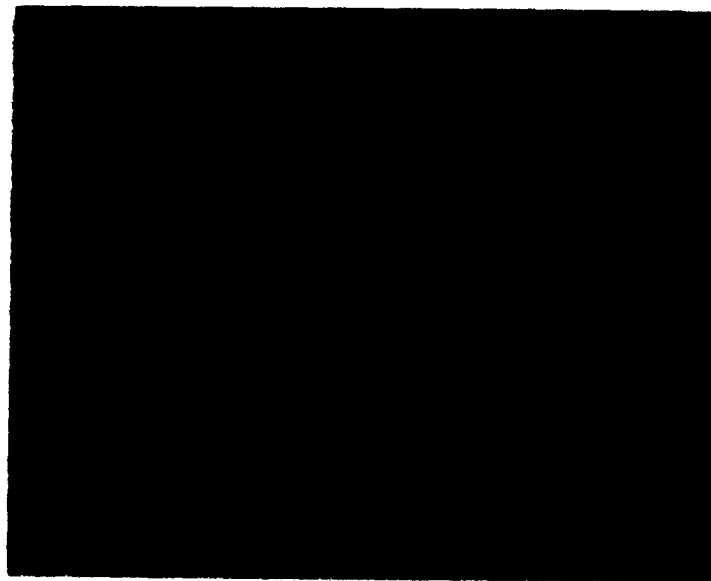
It is stated in Chapter III that a value of  $\Delta f$  of 1 kHz is a lower limit for the PLL design used. The output signal shown in Figure 8 is for a  $\Delta f$  of 1 kHz. Notice that the output signal has random oscillations. These random oscillations are expected since the  $\Delta f$  is at the lower limit for the PLL design. The signal also contains random oscillations when  $\Delta f = 1.25$  kHz in Figure 9, but when  $\Delta f = 2.0$  kHz in Figure 10 the demodulated signal is stable and capture can be observed and measured.

When both signals have the same value of  $\Delta f$  and this value is varied, it can be seen that capture ratio increases with  $\Delta f$ . This is supported by Figure 18 on page 29 where message frequencies of 100 Hz and 75 Hz for channel A and B respectively are used. For small values of  $\Delta f$ , the capture ratio is approximately 0.5 dB. As the value of  $\Delta f$  is increased, capture ratio increases until  $\Delta f = 12$  kHz where the capture ratio is 8 dB. The notation A/B and B/A in this figure and later figures signifies that signal A is captured over signal B for A/B and vice versa for B/A. Curves for both are necessary since the message frequencies are not the same.

It is evident that the value of  $\Delta f$  of the dominant signal determines the capture ratio and the  $\Delta f$  of the suppressed or weaker signal has no effect on capture ratio. This fact is demonstrated by Figure 19 on page 30 through Figure 21 on page 32.

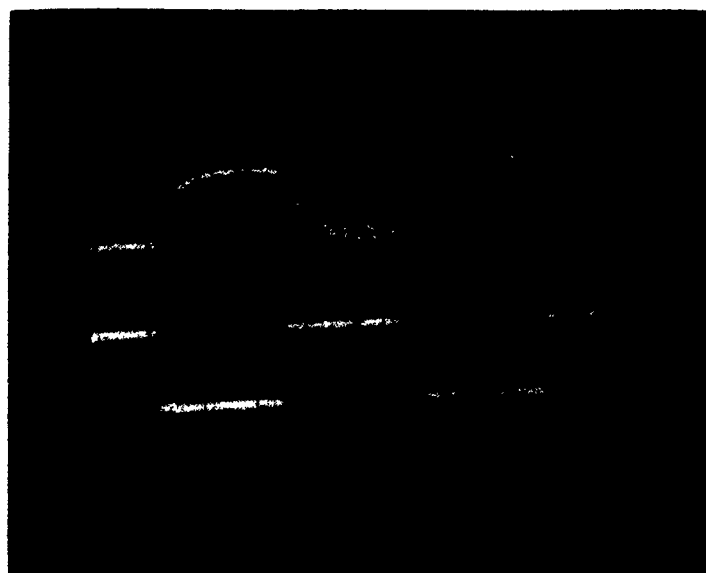


(a) Signal A Dominant.

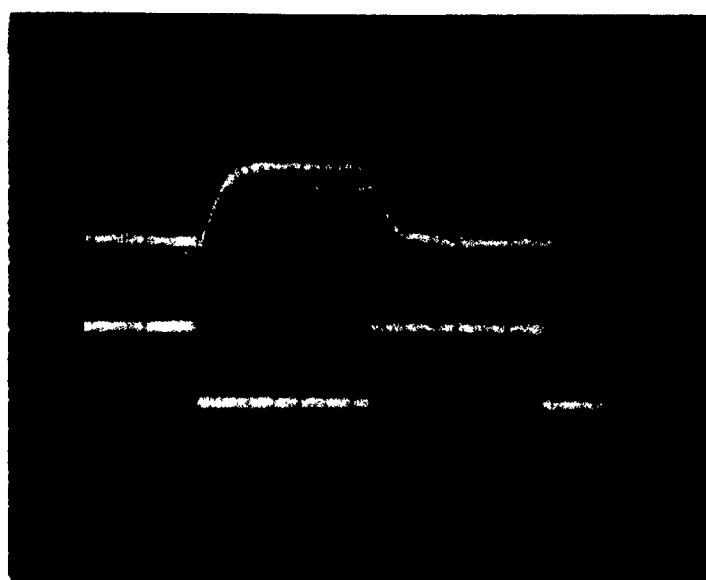


(b) Signal B Dominant.

**Figure 8. Demodulator Output (upper trace) and Message (lower trace) for Frequency Deviation of 1 kHz.**

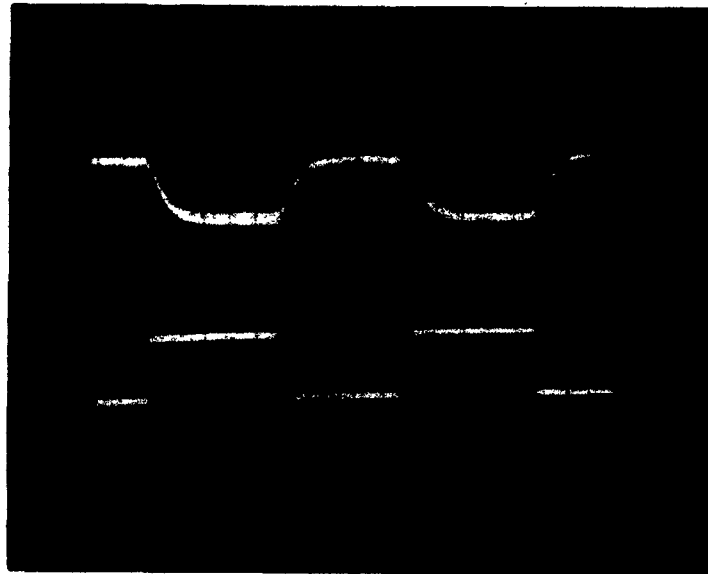


(a) Signal A Dominant.

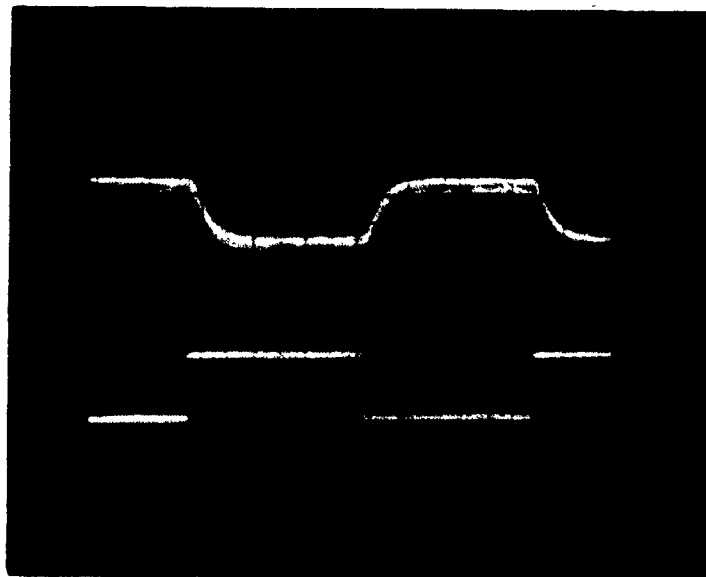


(b) Signal B Dominant.

**Figure 9. Demodulator Output (upper trace) and Message (lower trace) for Frequency Deviation of 1.25 kHz.**

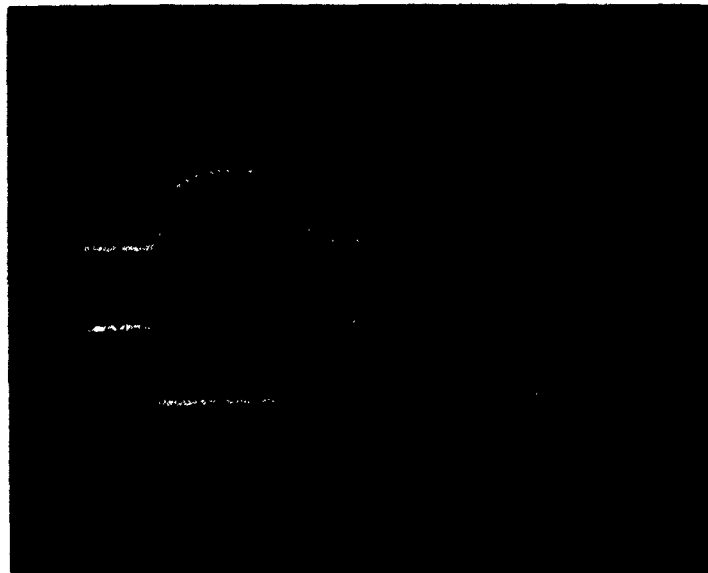


(a) Signal A Dominant.

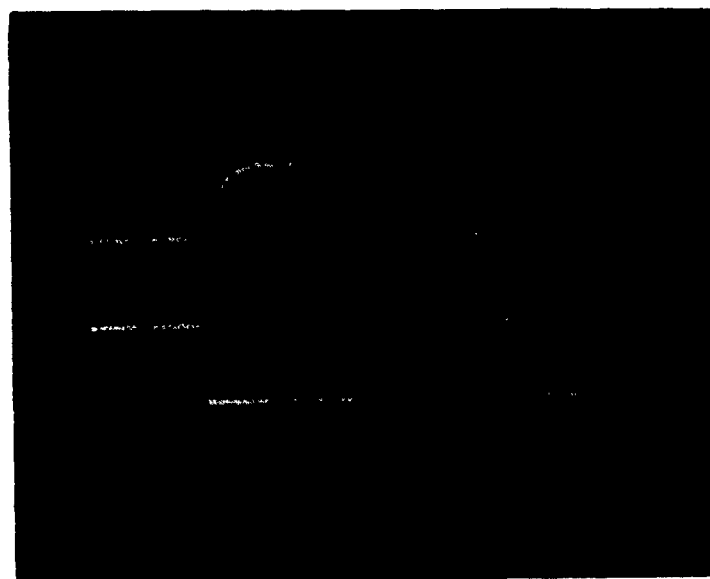


(b) Signal B Dominant.

**Figure 10. Demodulator Output (upper trace) and Message (lower trace) for Frequency Deviation of 2.0 kHz.**



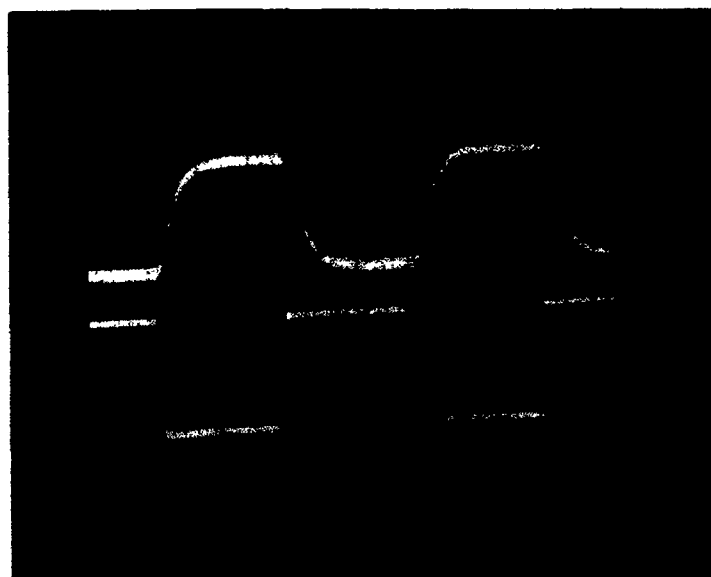
(a) Signal A Dominant.



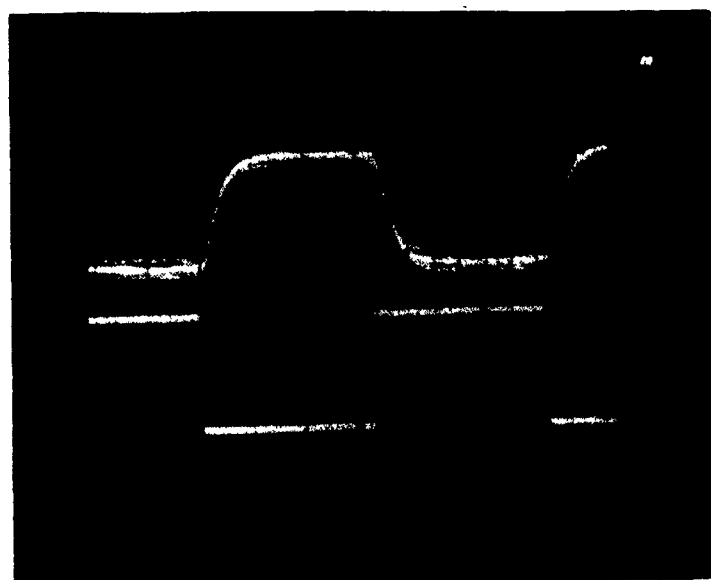
(b) Signal B Dominant.

Figure 11. Demodulator Output (upper trace) and Message (lower trace) for Frequency Deviation of 2.5 kHz.



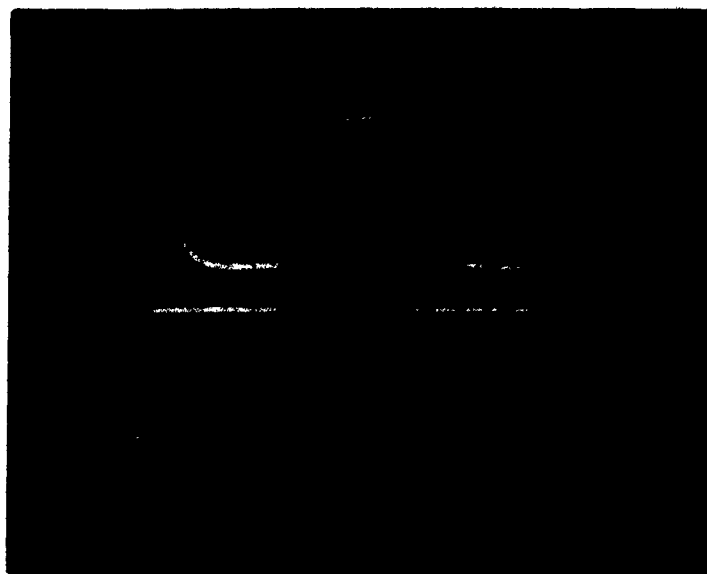


(a) Signal A Dominant.

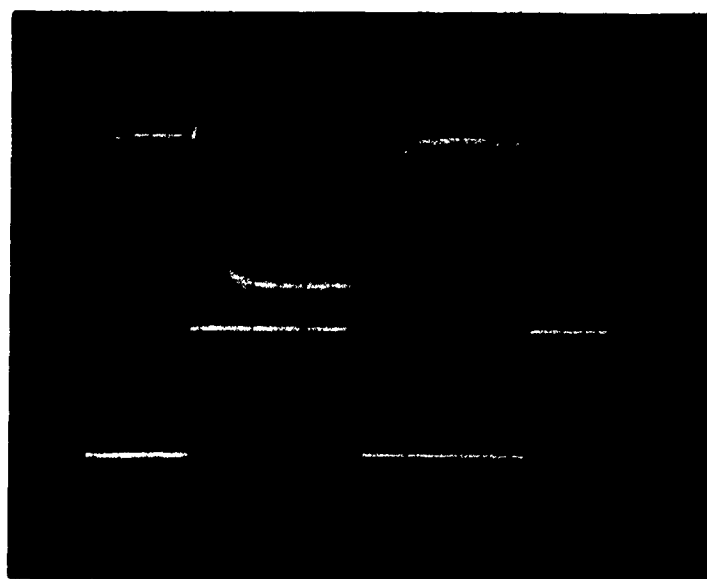


(b) Signal B Dominant.

Figure 12. Demodulator Output (upper trace) and Message (lower trace) for Frequency Deviation of 3.75 kHz.

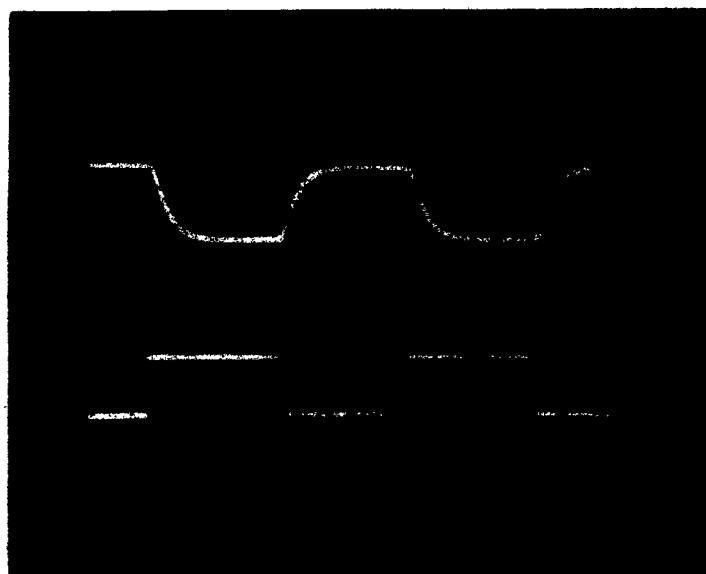


(a) Signal A Dominant.

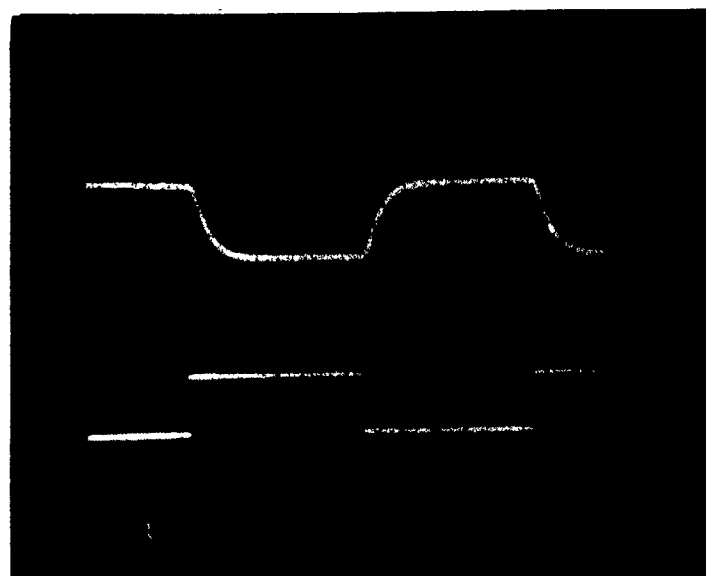


(b) Signal B Dominant.

Figure 13. Demodulator Output (upper trace) and Message (lower trace) for Frequency Deviation of 5.0 kHz.

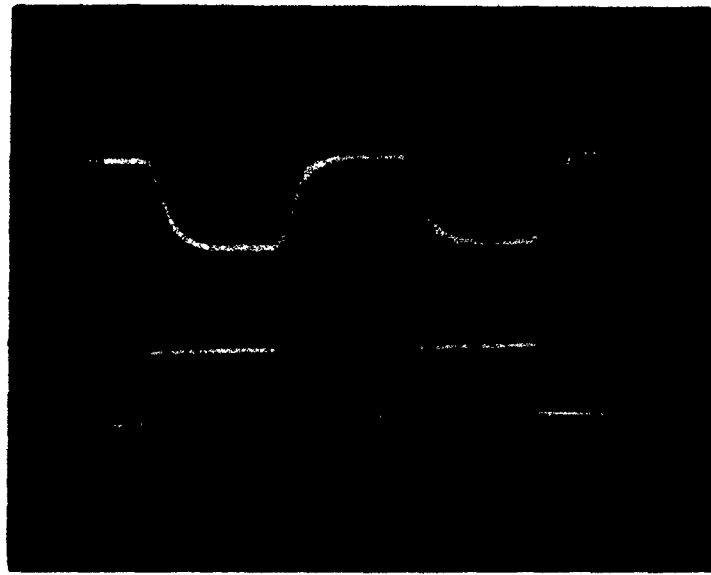


(a) Signal A Dominant.

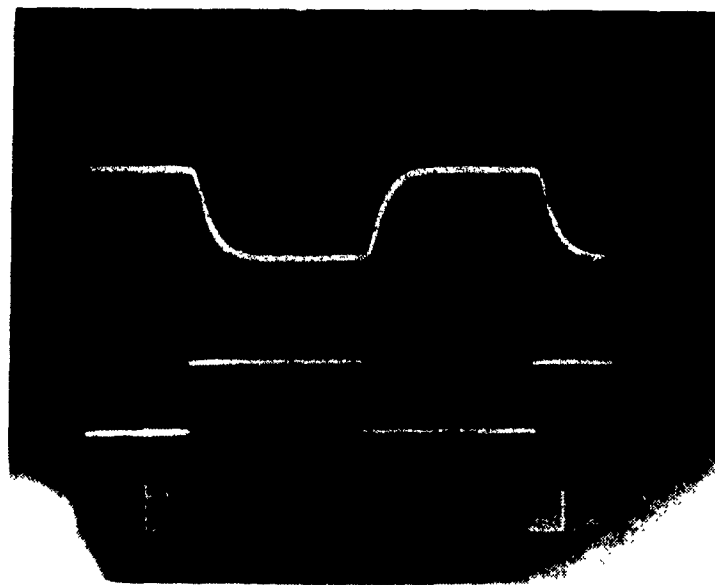


(b) Signal B Dominant.

**Figure 14. Demodulator Output (upper trace) and Message (lower trace) for Frequency Deviation of 6.25 kHz.**

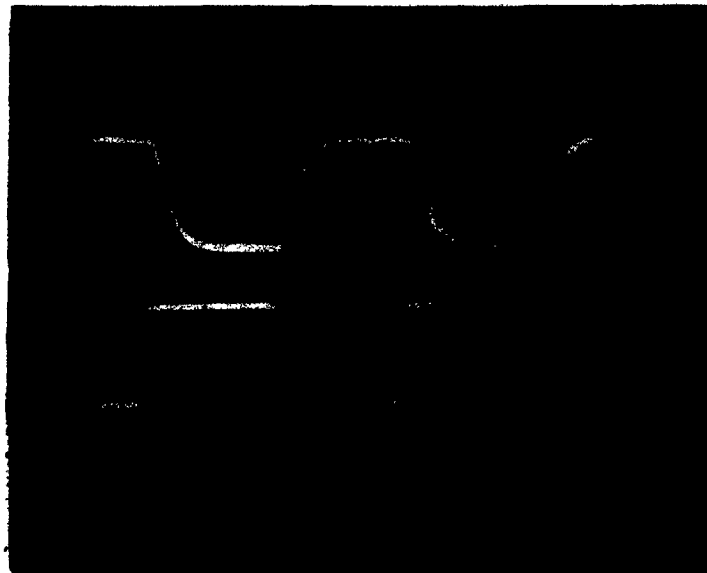


(a) Signal A Dominant.

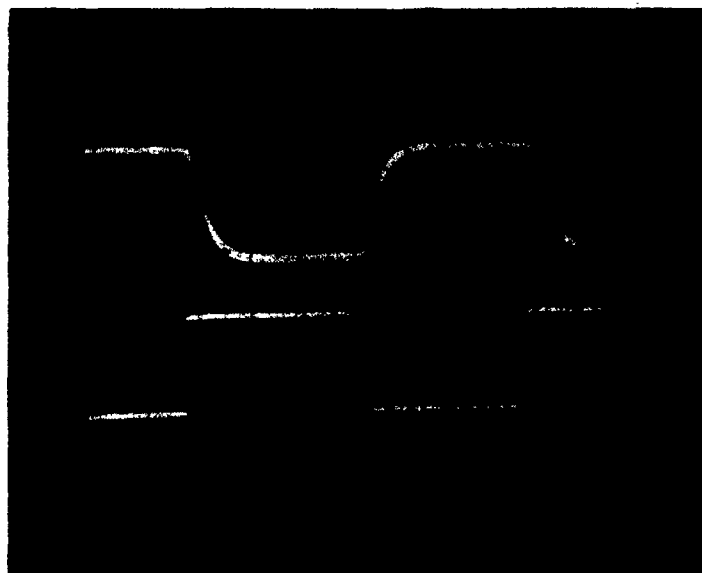


(b) Signal B Dominant.

**Figure 15. Demodulator Output (upper trace) and Message (lower trace) for Frequency Deviation of 7.5 kHz.**

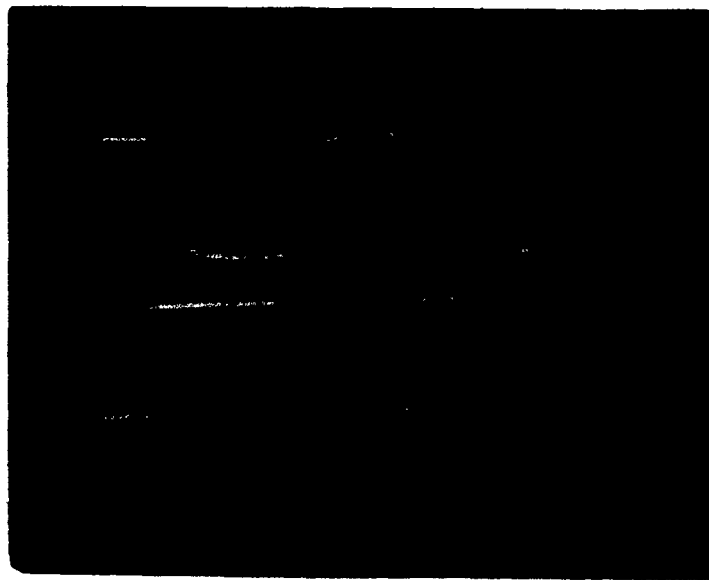


(a) Signal A Dominant.



(b) Signal B Dominant.

Figure 16. Demodulator Output (upper trace) and Message (lower trace) for Frequency Deviation of 8.75 kHz.



(a) Signal A Dominant.



(b) Signal B Dominant.

**Figure 17. Demodulator Output (upper trace) and Message (lower trace) for Frequency Deviation of 10.0 kHz.**

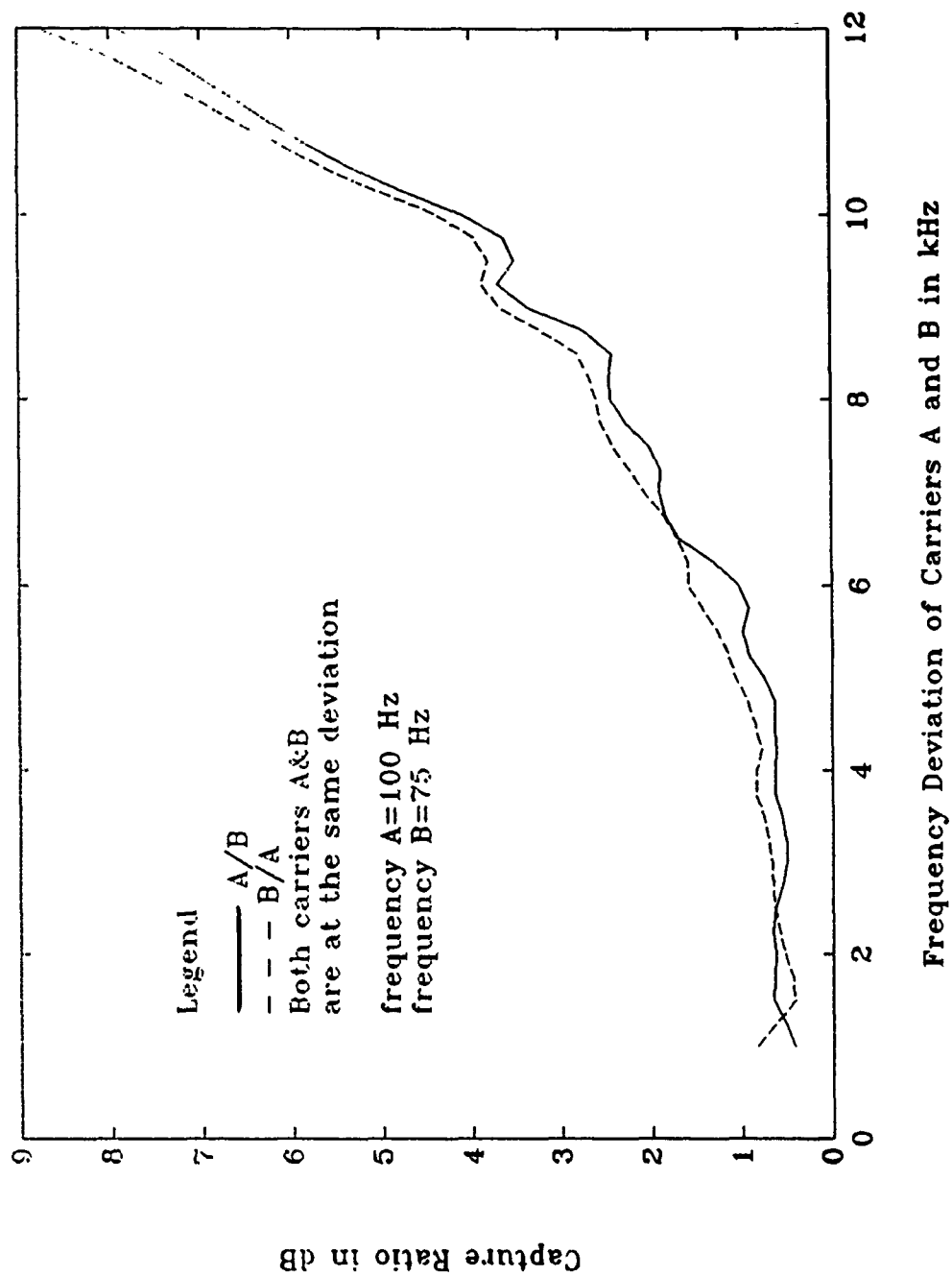
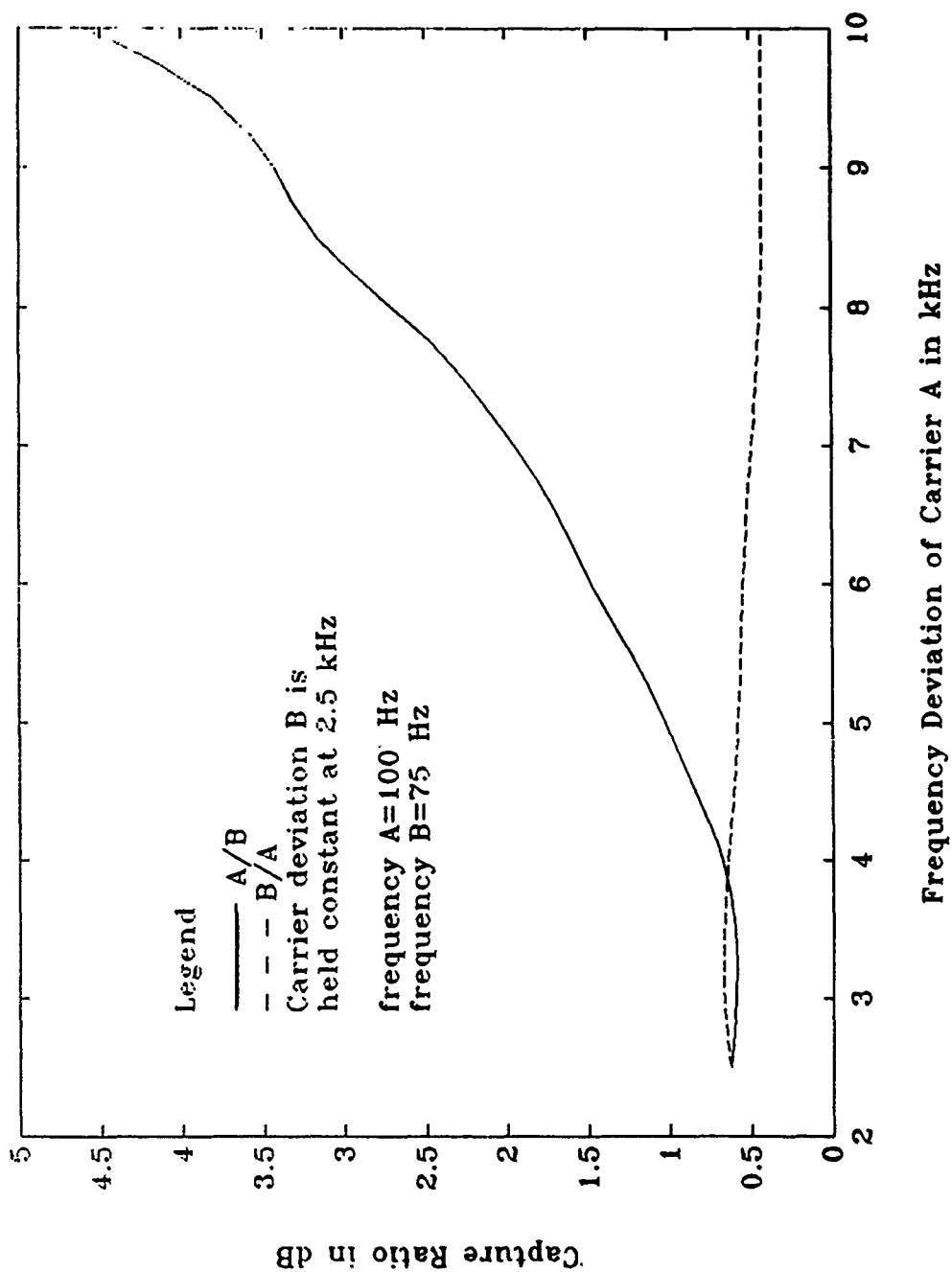


Figure 18. Capture Ratio vs. Frequency Deviation of Carriers A and B.



**Figure 19. Capture Ratio vs. Frequency Deviation of Carrier A when the Frequency Deviation of Carrier B is 2.5 kHz.**



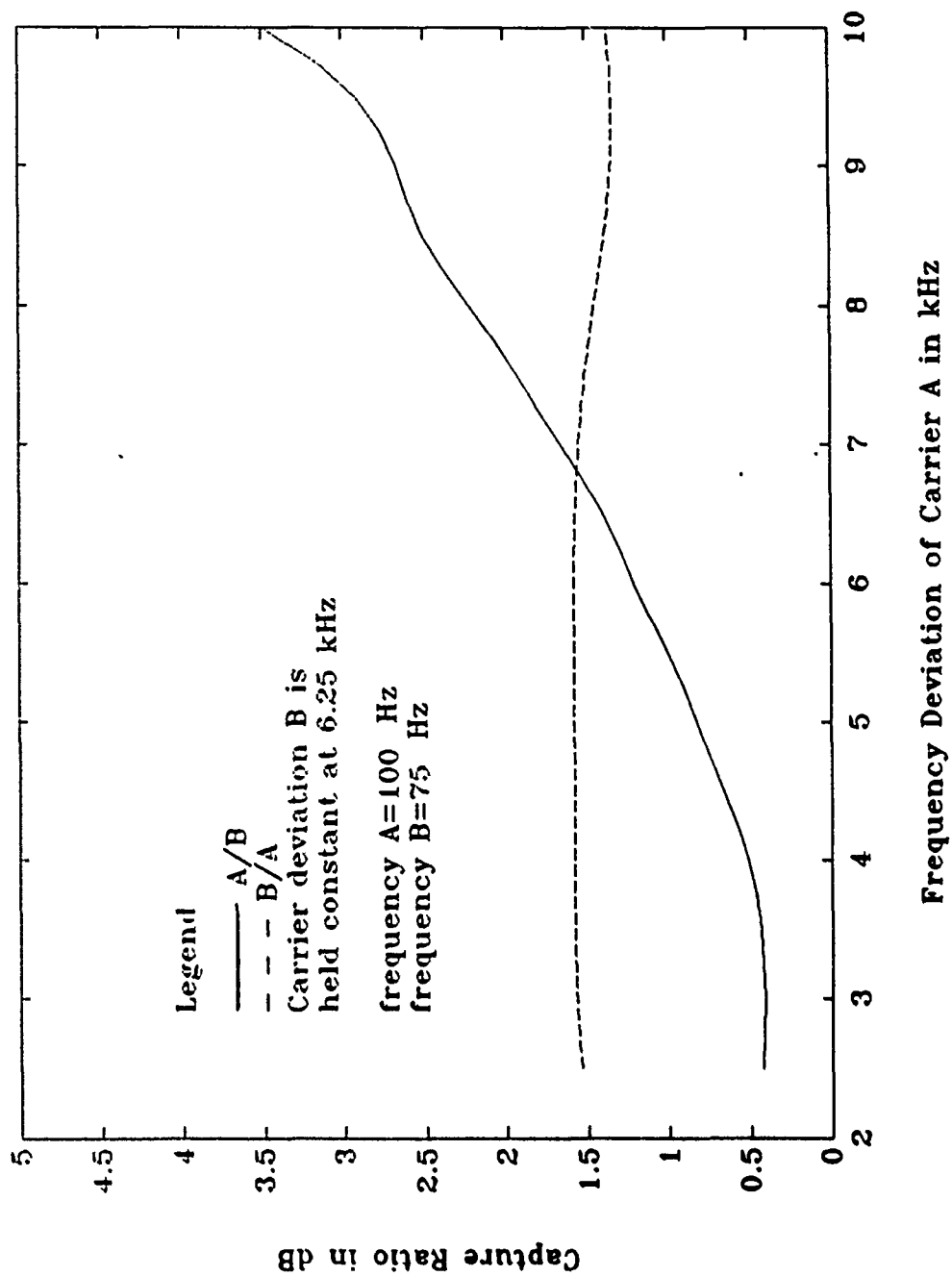


Figure 20. Capture Ratio vs. Frequency Deviation of Carrier A when the Frequency Deviation of Carrier B is 6.25 kHz.

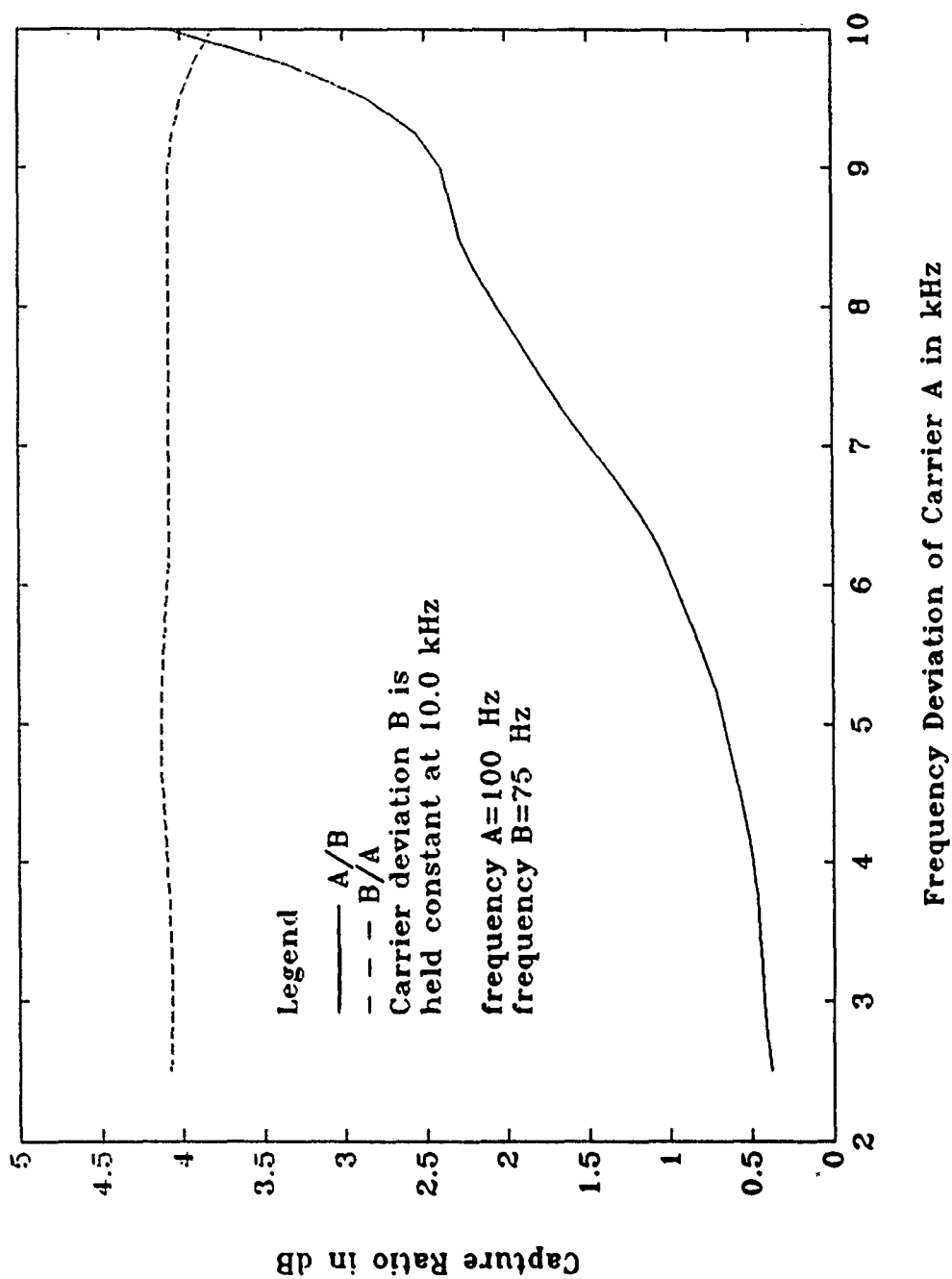


Figure 21. Capture Ratio vs. Frequency Deviation of Carrier A when the Frequency Deviation of Carrier B is 10.0 kHz.

In these figures,  $\Delta f$  of signal B is held constant at three different values. These values are 2.5 kHz, 6.25 kHz and 10.0 kHz. There is a plot for each of these cases. In each plot it can be seen that the capture ratio for the constant signal (signal B) remains steady. This is seen by the behavior of the curve B/A in each of these plots. The capture ratio of the signal whose  $\Delta f$  changes (signal A) follows the same pattern as seen in Figure 18. This is seen by the behavior of the curve A/B in each of these plots. For larger values of  $\Delta f$ , a larger value of capture ratio is required.

To further demonstrate how the capture ratio is unaffected by  $\Delta f$  of the weaker signal, a plot is made by replotting the capture ratios A/B from Figure 19 through Figure 21 onto a separate plot in Figure 22 on page 34. Notice that all three curves in this figure follow the same pattern. Each curve has a different value of  $\Delta f$  for the weaker signal (signal B); yet, they are similar. This reemphasizes that the capture ratio is unaffected by the frequency deviation of the weaker signal.

To restate the results for the parameter  $\Delta f$ , the capture ratio required depends on the  $\Delta f$  of the dominant (stronger) signal and is independent of that of the suppressed (weaker) signal.

## B. SIGNAL FREQUENCY

The next set of data is similar to that taken for the parameter  $\Delta f$ , but at larger values of message frequencies. The frequency of message A is set at 400 Hz and the frequency of message B is set at 60 Hz. A plot is made of capture ratio vs.  $\Delta f$  for the case where both signal A and B have the same  $\Delta f$  and  $\Delta f$  is varied. Also, plots are made for the case where signal B has a constant value of  $\Delta f$  while the value of  $\Delta f$  for signal A is varied.

As before, photographs are provided to demonstrate the signal appearance when capture occurs. Figures 23 through 25 show the output when the dominant message at the demodulator output is a square wave at 400 Hz and 60 Hz for  $\Delta f$  ranging from 3 kHz to 7 kHz. It is evident that the signals are stable and unperturbed by the suppressed (weaker) signal.

The graph of capture ratio vs.  $\Delta f$  where signal A and B have the same value of  $\Delta f$  is shown in Figure 26 on page 38. The capture ratio required follows the same pattern and is roughly the same magnitude as that for the case of Figure 18 where the frequency of signals A and B are 100 Hz and 75 Hz respectively. It appears that the frequency of the message has negligible effect on the capture ratio.

Plots of capture ratio for the cases where the value of  $\Delta f$  for signal B is held constant at 2.5 kHz, 6.25 kHz and 10 kHz while the value of  $\Delta f$  for signal A is varied are given

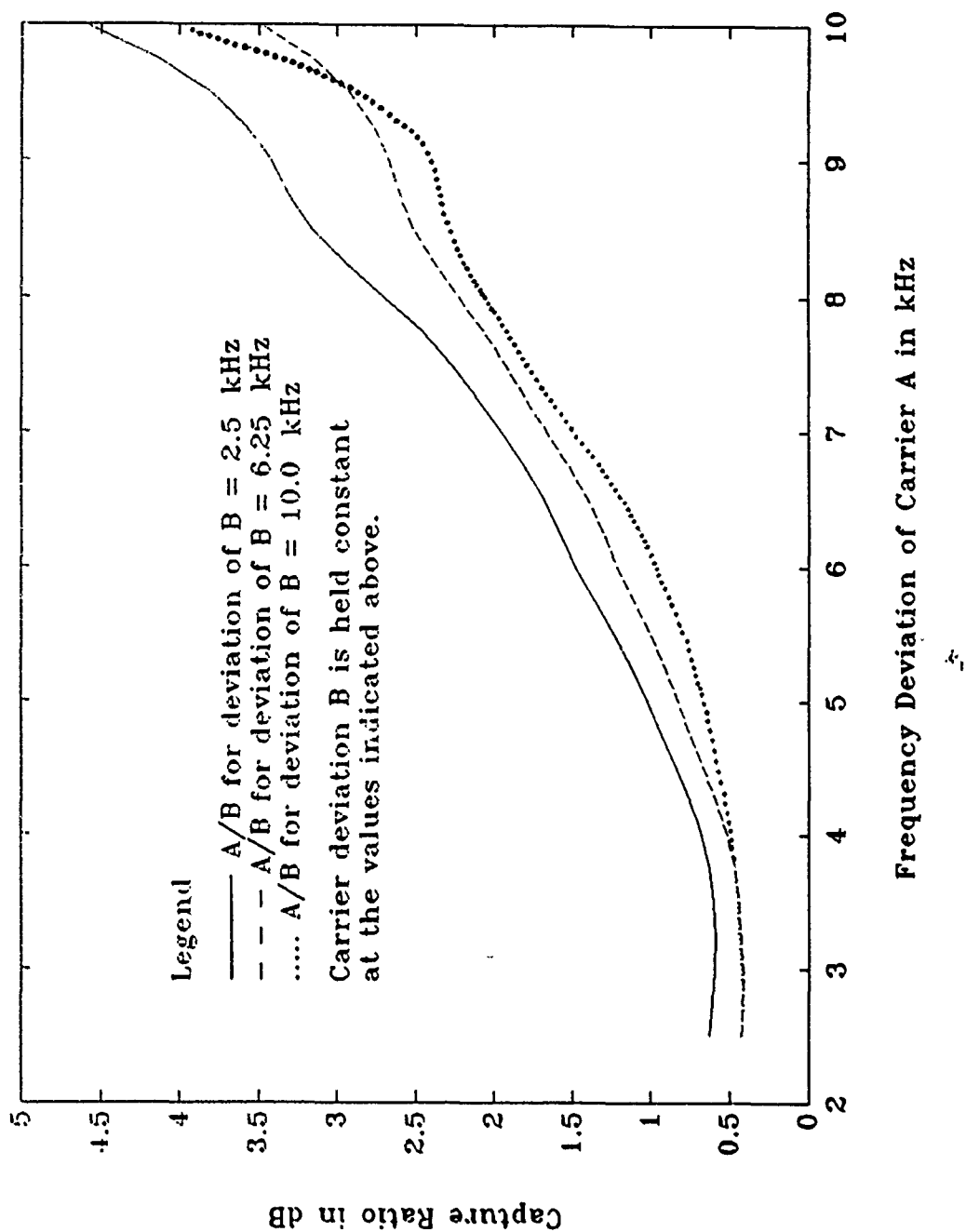
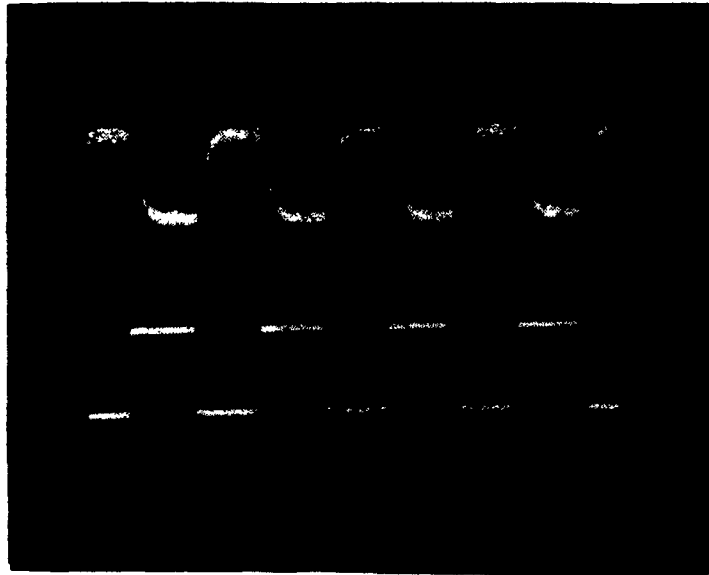
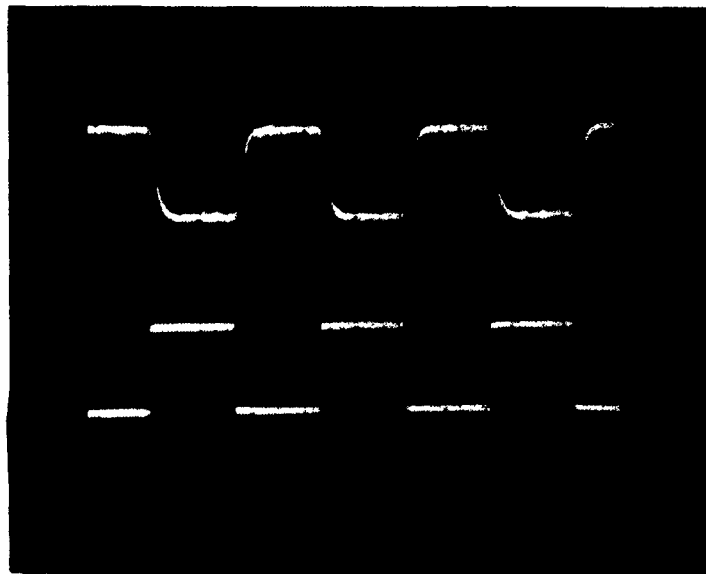


Figure 22. Capture Ratio (A/B) vs. Frequency Deviation of Carrier A where the Frequency Deviation of B is 2.5, 6.25 and 10.0 kHz.

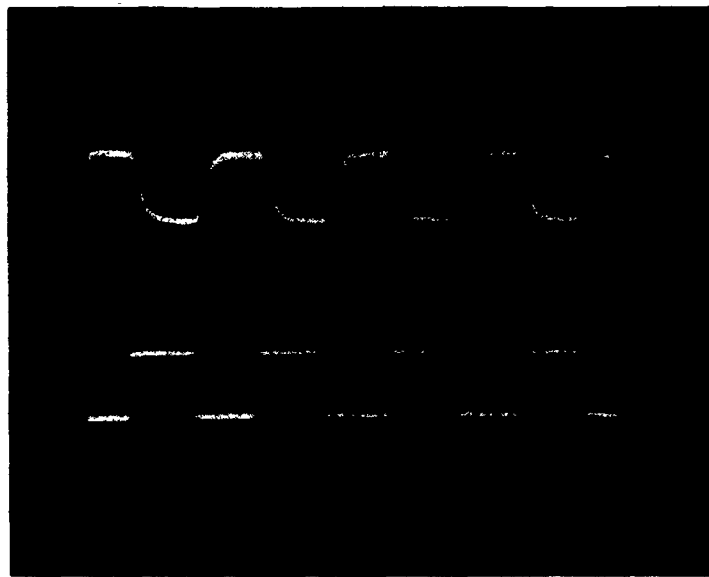


(a) Signal A Dominant.

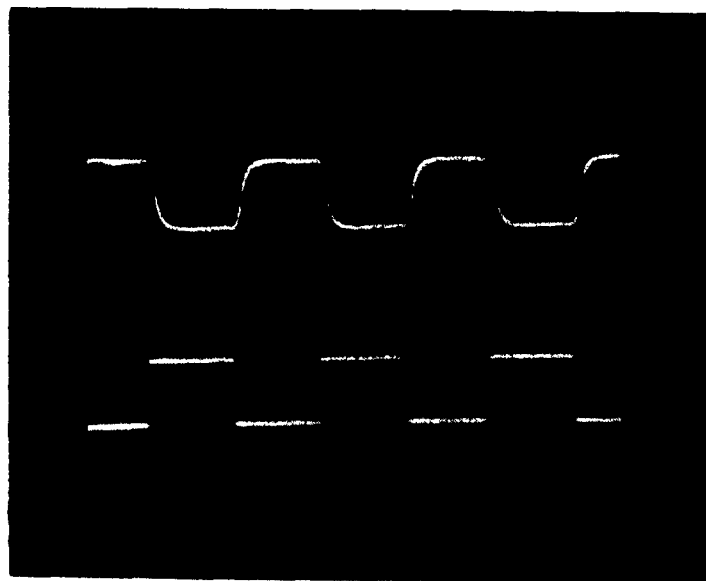


(b) Signal B Dominant.

**Figure 23. Demodulator Output (upper trace) and Message (lower trace) for Frequency Deviation of 3 kHz.**



(a) Signal A Dominant.

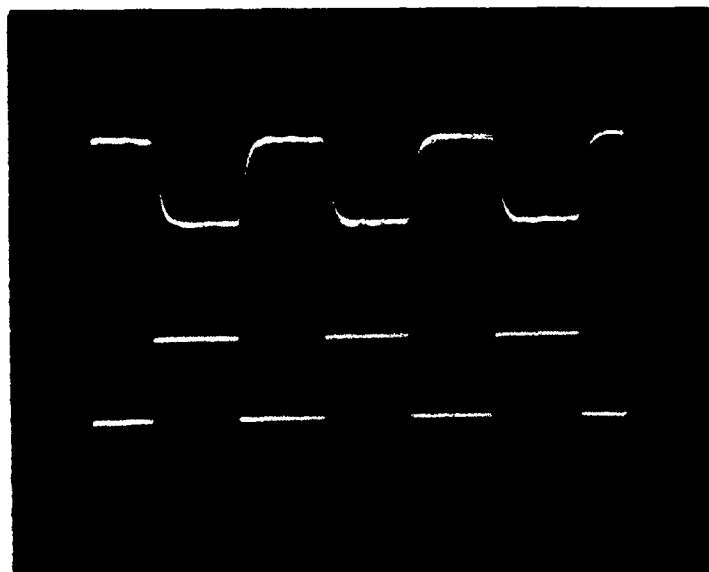


(b) Signal B Dominant.

Figure 24. Demodulator Output (upper trace) and Message (lower trace) for Frequency Deviation of 5.5 kHz.



(a) Signal A Dominant.



(b) Signal B Dominant.

**Figure 25. Demodulator Output (upper trace) and Message (lower trace) for Frequency Deviation of 7 kHz.**

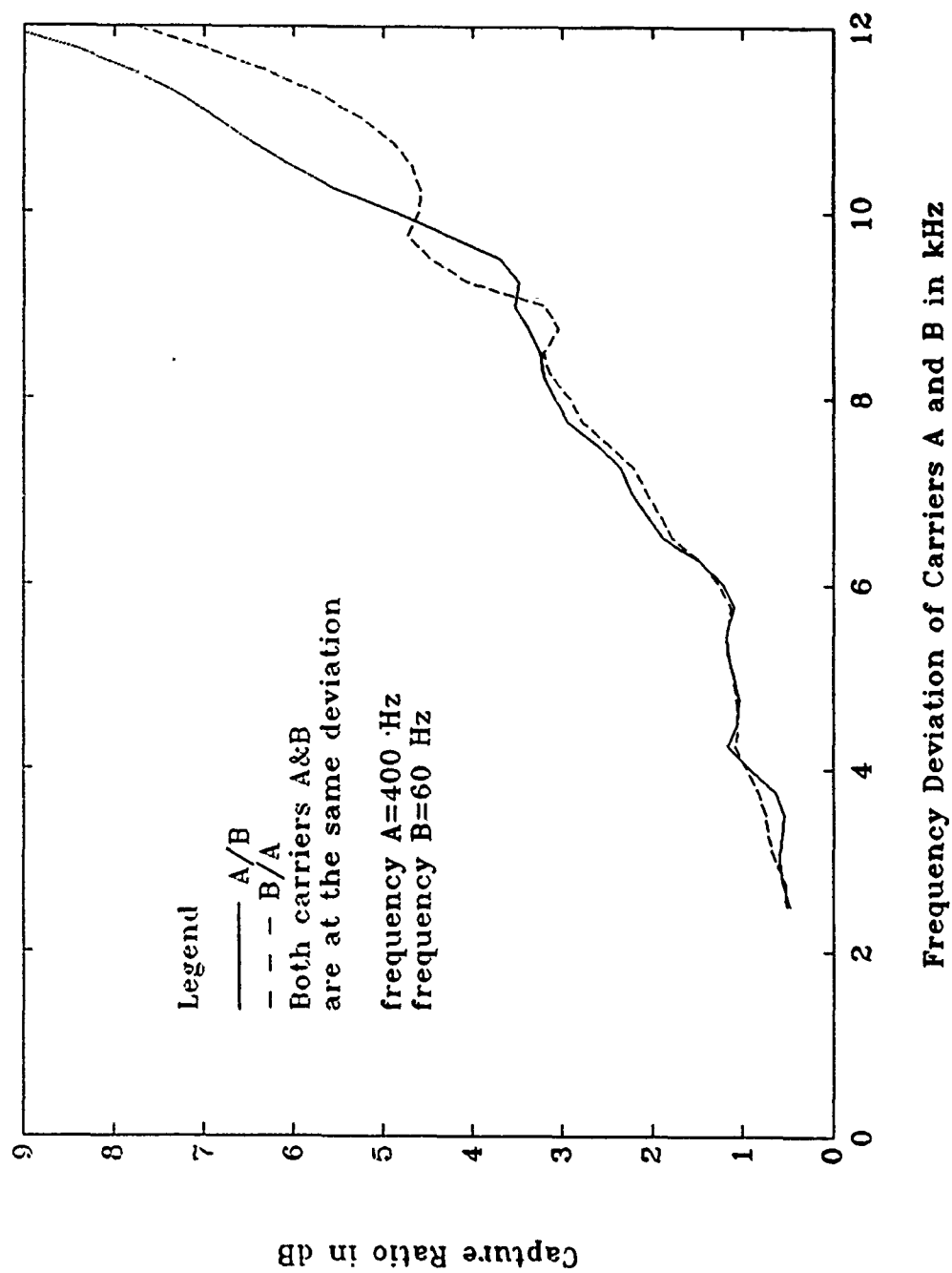


Figure 26. Capture Ratio vs. Frequency Deviation of Carriers A and B.



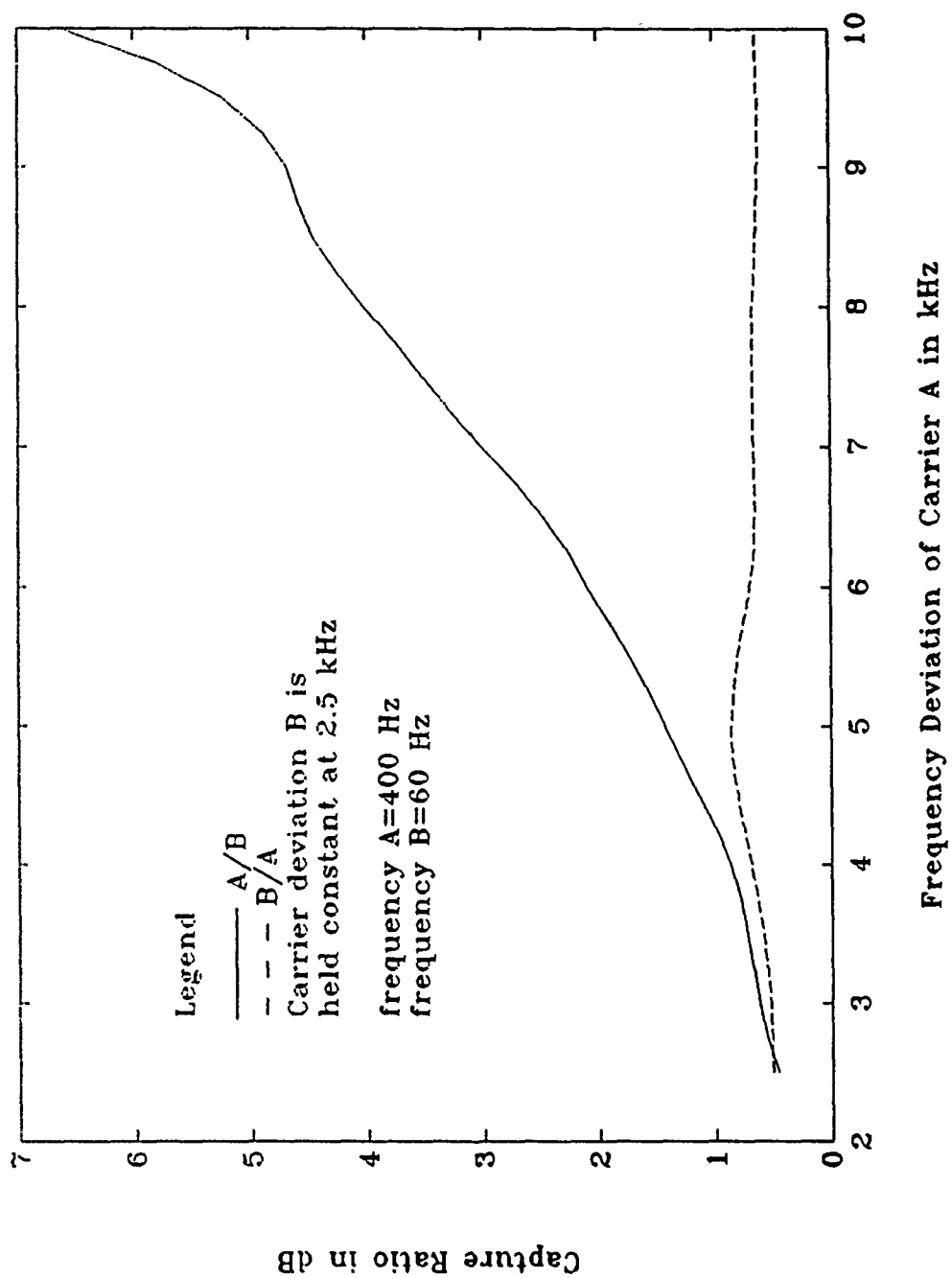


Figure 27. Capture Ratio vs. Frequency Deviation of Carrier A when the Frequency Deviation of B is 2.5 kHz.

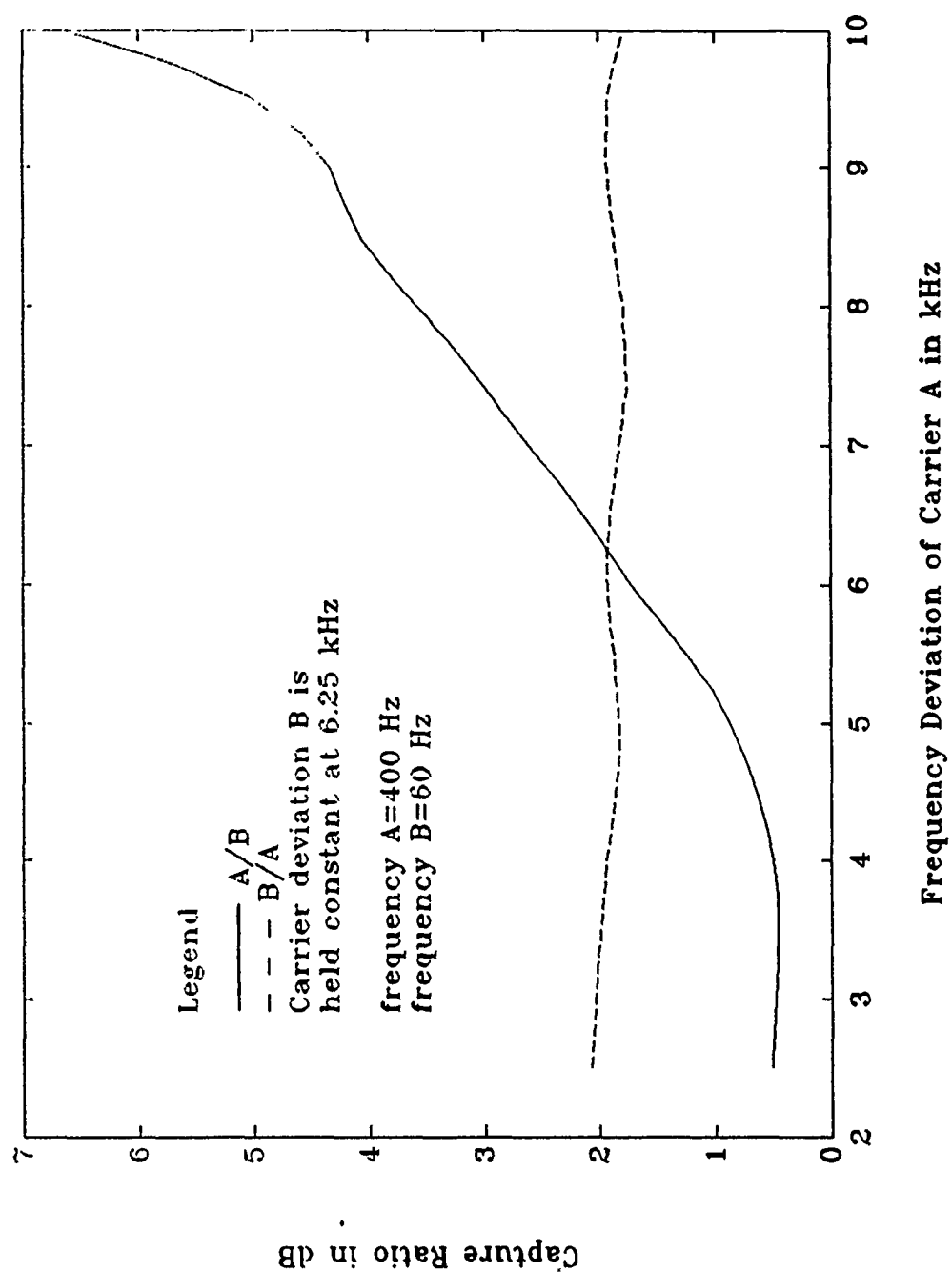


Figure 28. Capture Ratio vs. Frequency Deviation of Carrier A when the Frequency Deviation of B is 6.25 kHz.

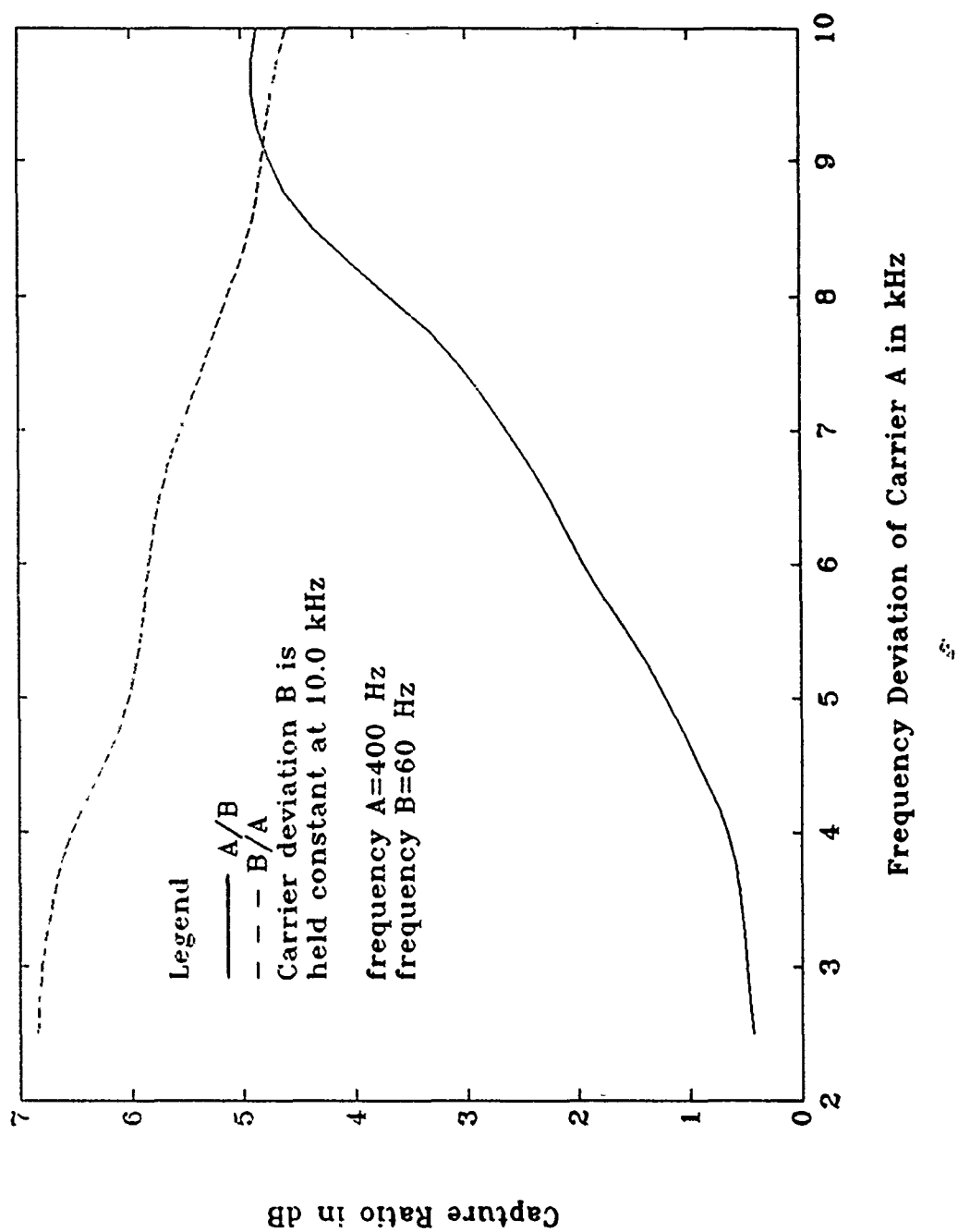


Figure 29. Capture Ratio vs. Frequency Deviation of Carrier A when the Frequency Deviation of B is 10.0 kHz.

in Figures 27 through 29. It again can be seen that the capture ratio of the stronger signal is dependent on  $\Delta f$  of the stronger signal and independent of  $\Delta f$  of the weaker signal. The curves look similar to those for frequencies A and B equal 100 Hz and 75 Hz respectively plotted in Figures 19 through 21. To see the effect of message frequency on the capture ratio, the values of A/B when  $\Delta f$  of signal B is held constant at three distinct values is compared to the two different message frequency cases. The capture ratios of A/B for the case of  $f_A = 100\text{Hz}$  and  $f_B = 75\text{ Hz}$  from Figures 19 through 21 are plotted with A/B for  $f_A = 400\text{ Hz}$  and  $f_B = 60\text{ Hz}$ . This is done in Figures 30 through 32. Observing these plots it can be seen that the capture ratio curve for the messages of higher frequency (400 Hz) consistently lies above the capture ratio curve for the message of lower frequency (100 Hz). This shows a dependance of capture ratio on the message frequency.

Based on the manipulations required to observe the dependance of capture ratio on message frequency, we can only determine that some slight increase in capture ratio required occurs as the message frequency of the captured signal is increased. Also note from Figures 30 through 32 that this required increase grows with  $\Delta f$ . This is not a pronounced effect.

### C. PLL FILTER BANDWIDTH AND DESIGN

The final parameter that is analyzed is the PLL loop filter bandwidth and design. As described in Appendix B, the filter bandwidths of each design are kept equal as both are varied from 3 kHz to infinity. The lag-lead filter outperformed the lag filter at the lower bandwidths and both filters performed the same for higher bandwidths.

The best explanation of increased performance by the lag-lead filter can be given by observing the Photographs in Figure 33 on page 46 and Figure 34 on page 47. These photographs show the filter output for both square wave and sine wave messages for the lag-lead as well as the lag configuration. It is evident that the lag filter has a larger random-appearing component in its output. The higher frequencies in the lag filter are attenuated less than in the lag-lead filter. In the lag-lead filter we can see that the signal splits and the higher frequencies are limited to oscillations between the two signals. The amplitude level of the split signal is smoother than the amplitude level of the signal for the lag filter case. It is easier to filter out the low pass signal from the less distorted lag-lead output.

The effect of the filter design and bandwidth on capture ratio is seen in Figures 35 through 38. These figures show the capture ratio of the messages vs. the bandwidth of

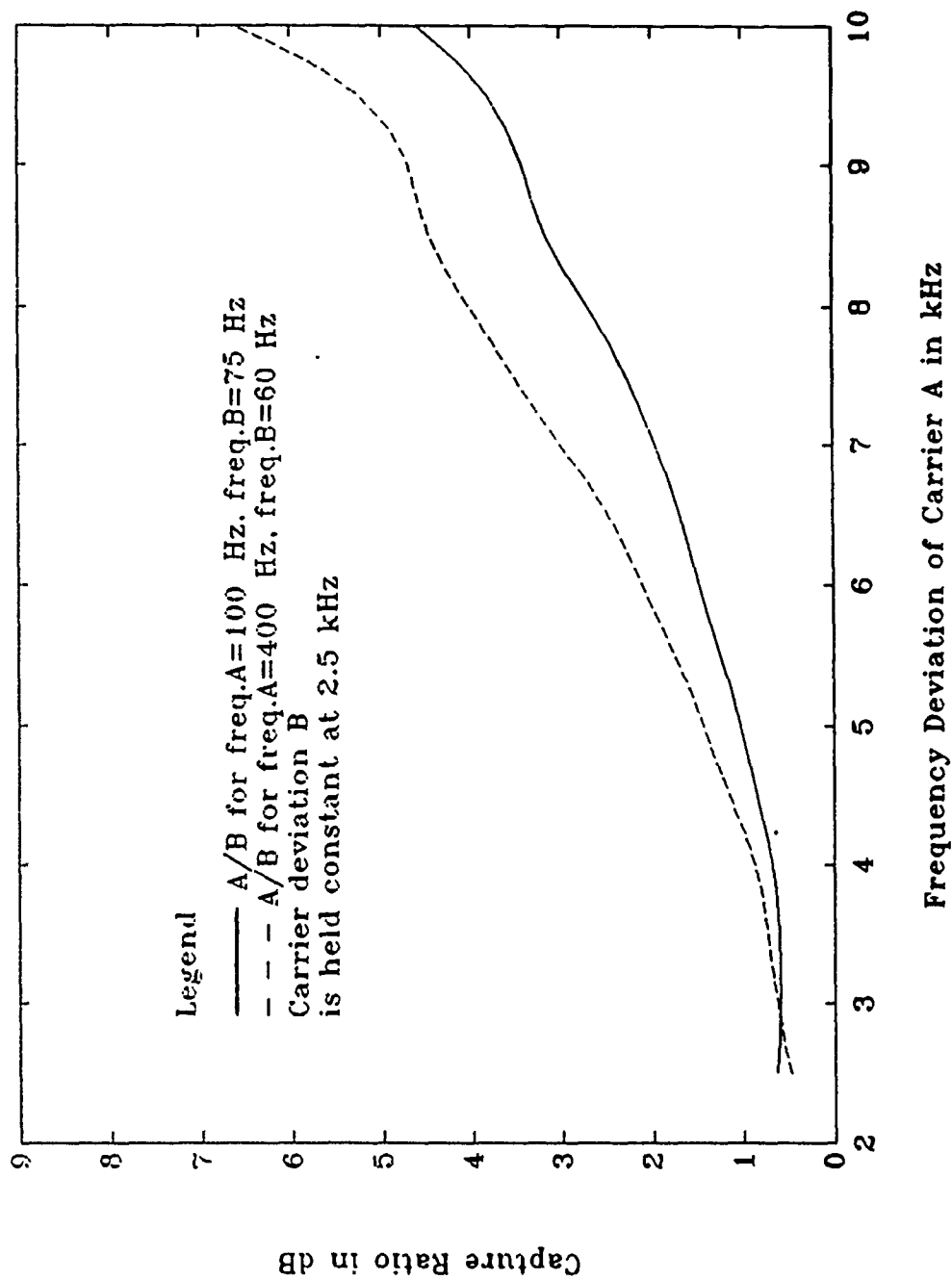


Figure 30. Capture Ratio (A/B) vs. Frequency Deviation of Carrier A when the Frequency Deviation of B is 2.5 kHz.

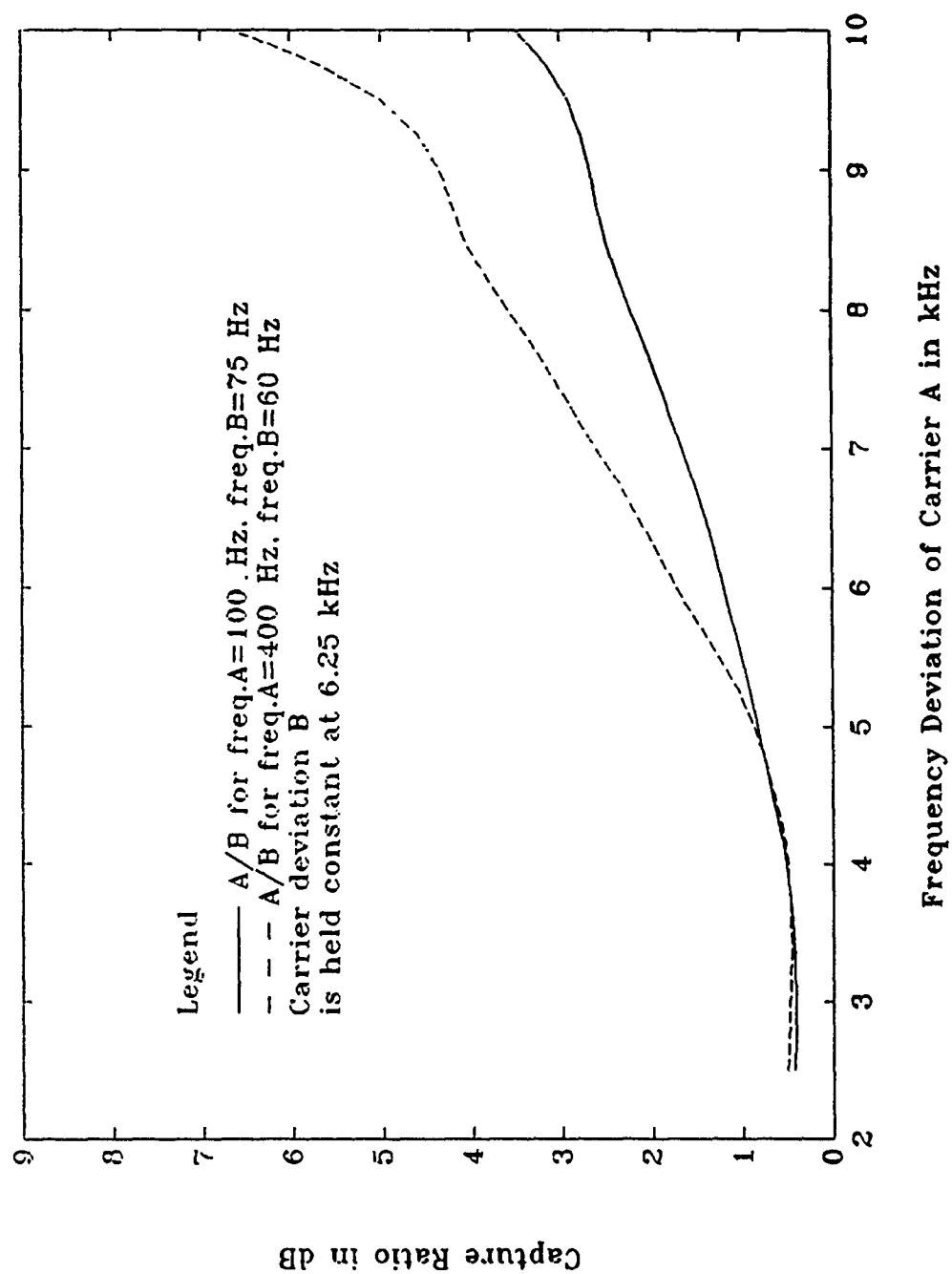
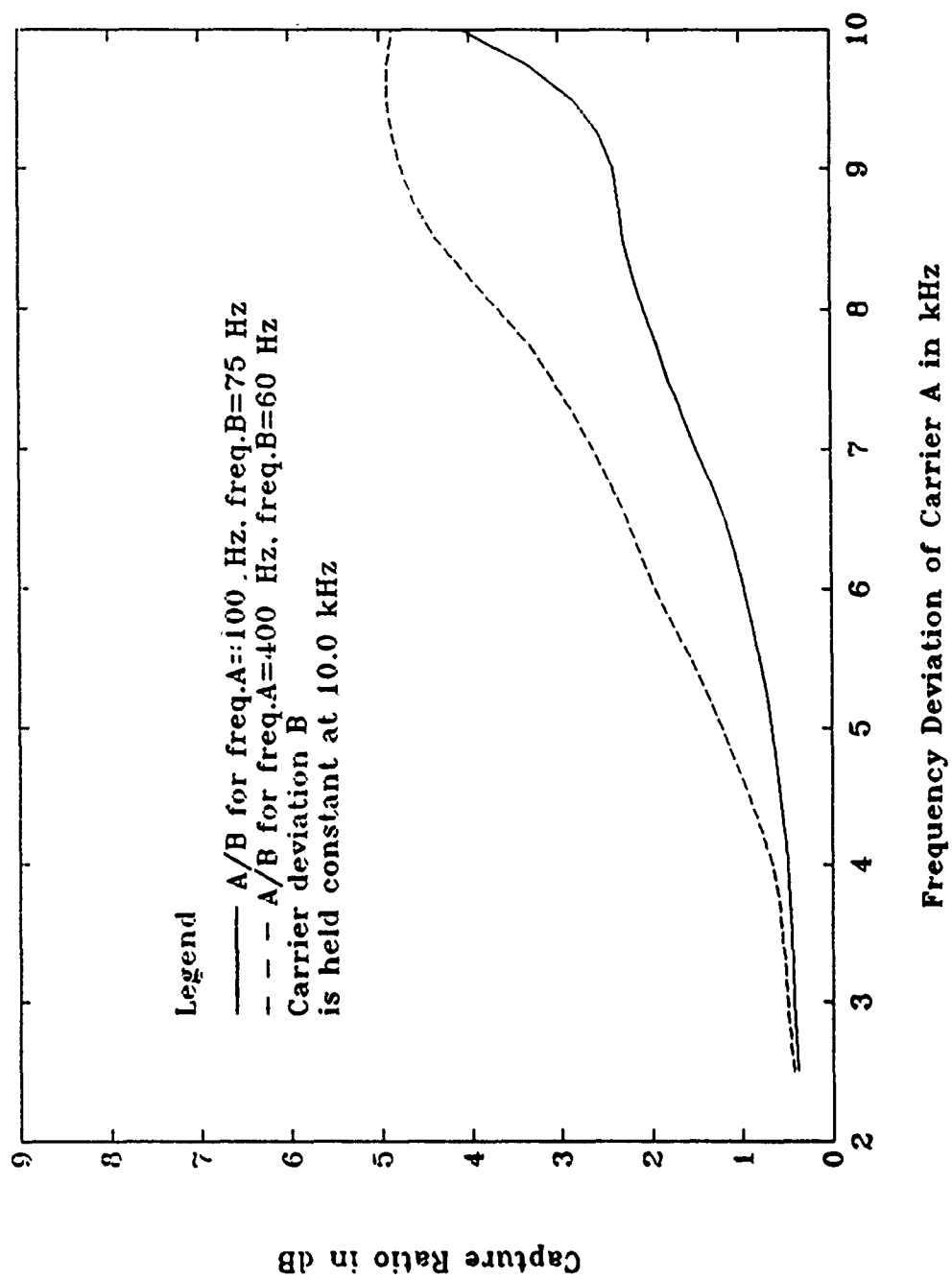
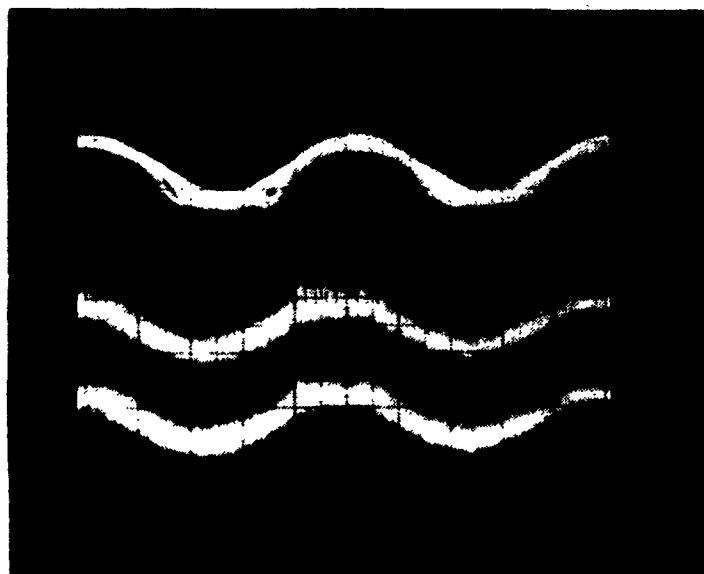


Figure 31. Capture Ratio (A/B) vs. Frequency Deviation of Carrier A when the Frequency Deviation of B is 6.25 kHz.



**Figure 32. Capture Ratio (A/B) vs. Frequency Deviation of Carrier A when the Frequency Deviation of B is 10.0 kHz.**



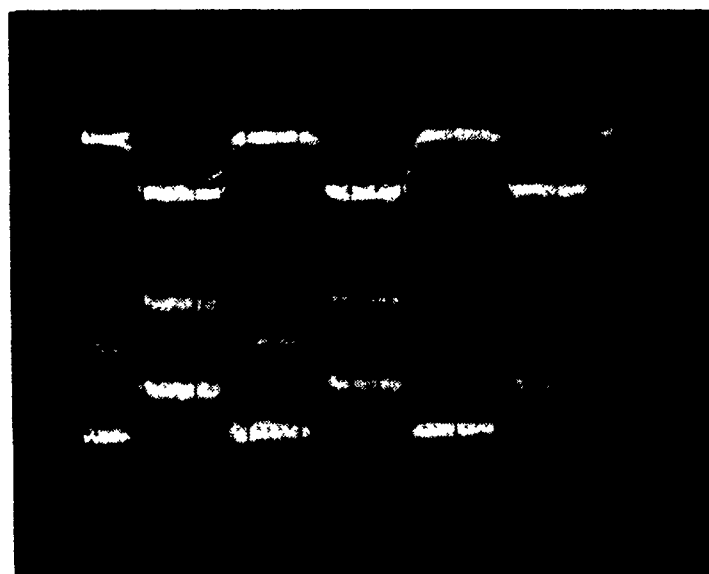
(a) Lag-Lead Filter.



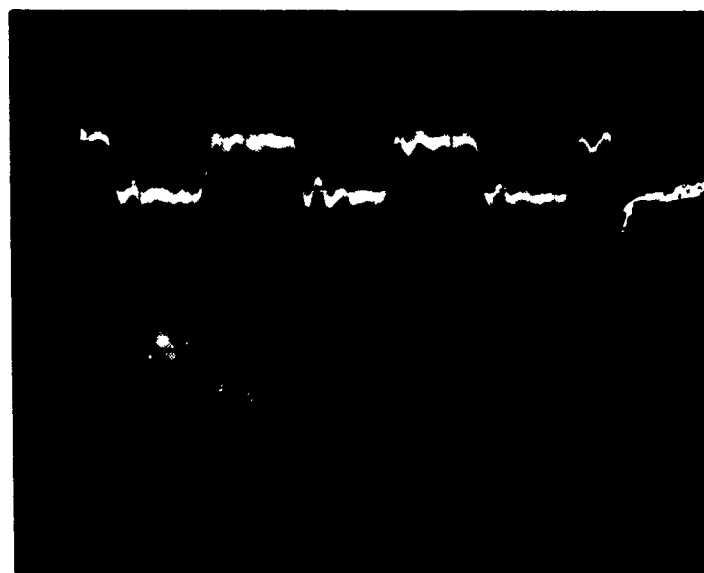
(b) Lag Filter.

Figure 33. PLL Loop Filter Output (lower trace) and Post Detection Filter Output (upper trace) for Sine Wave Message.





(a) Lag-Lead Filter.



(b) Lag Filter.

Figure 34. PLL Loop Filter Output (lower trace) and Post Detection Filter Output (upper trace) for Square Wave Message.

the loop filter for both the lag-lead and the lag configurations. For these curves a triangle wave was used as the message with  $f_a = 300$  Hz and  $f_b = 100$  Hz. The value of  $\Delta f$  for both the signals was held constant at 5.0 kHz for the first two figures and at 1.0 kHz for the last two figures.

For all cases the lag-lead requires smaller values of capture ratio at smaller bandwidths. Both filters perform the same at bandwidths greater than 20 kHz. The value of  $\Delta f$  of 1.0 kHz requires smaller values of capture ratio and the lag filter approaches the performance of the lag-lead filter more rapidly (at 6 kHz vice 20 kHz).

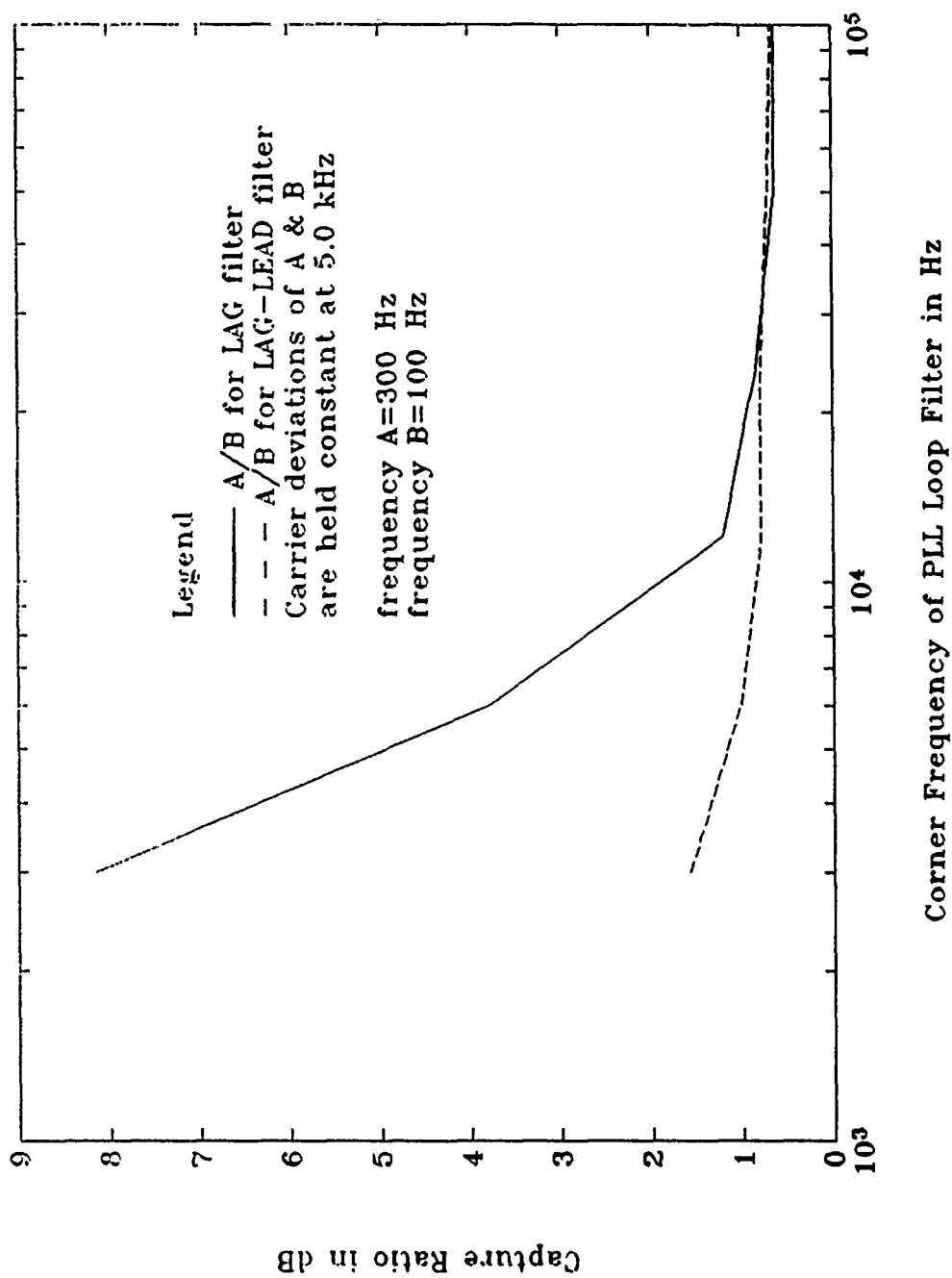


Figure 35. Capture Ratio (A/B) vs. Bandwidth of PLL Loop Filter.

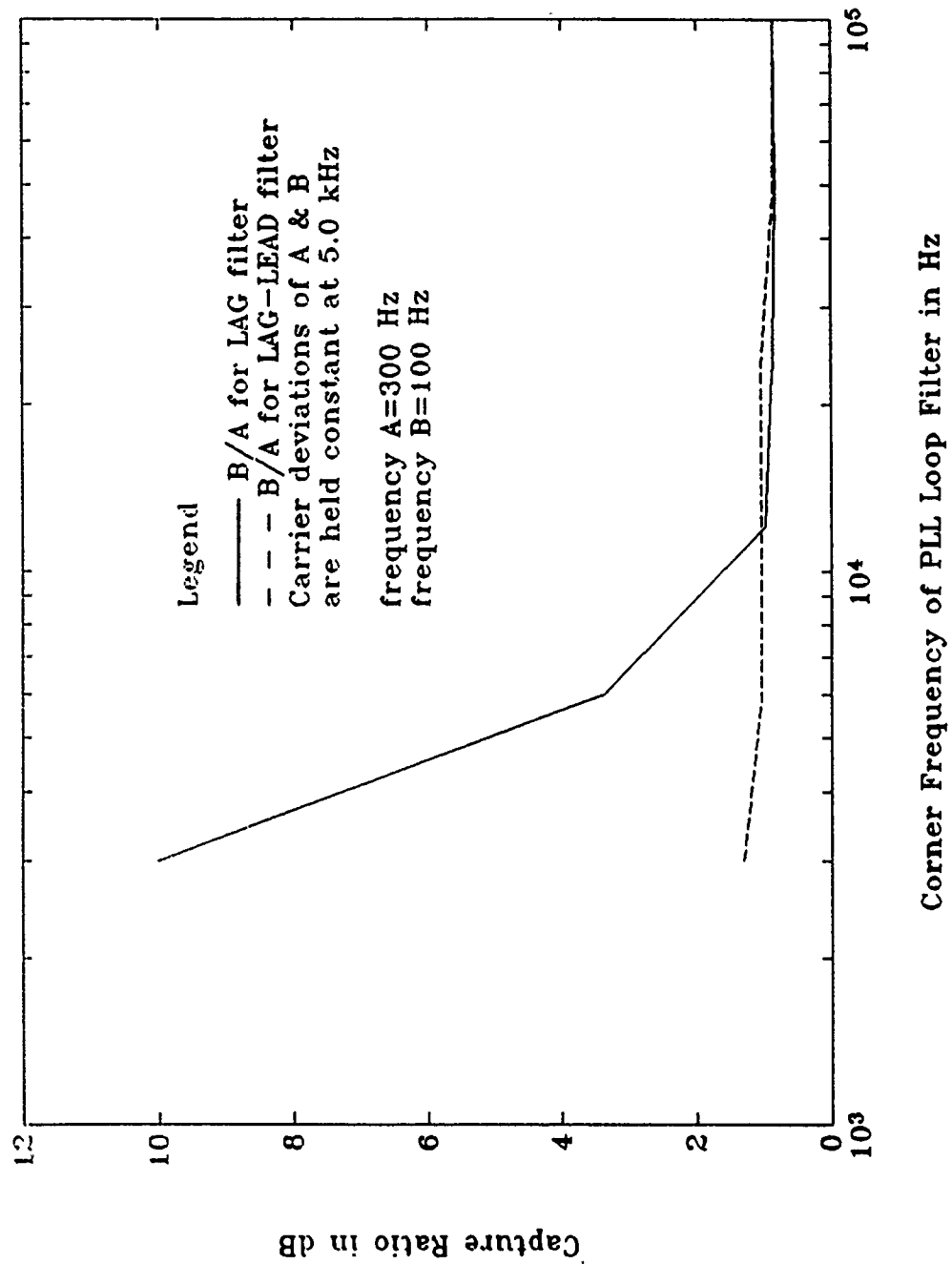


Figure 36. Capture Ratio (B/A) vs. Bandwidth of PLL Loop Filter.

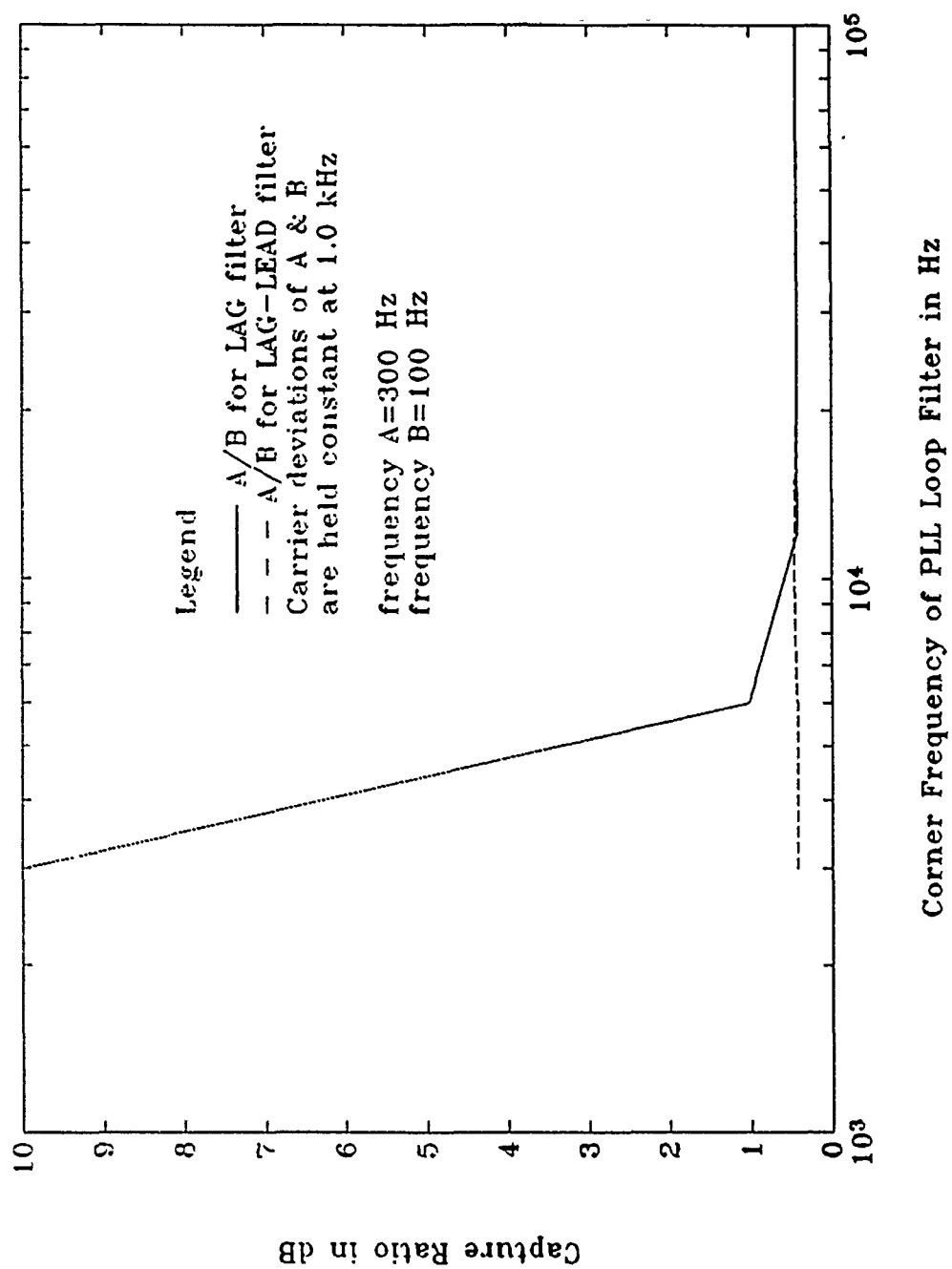


Figure 37. Capture Ratio (A/B) vs. Bandwidth of PLL Loop Filter.

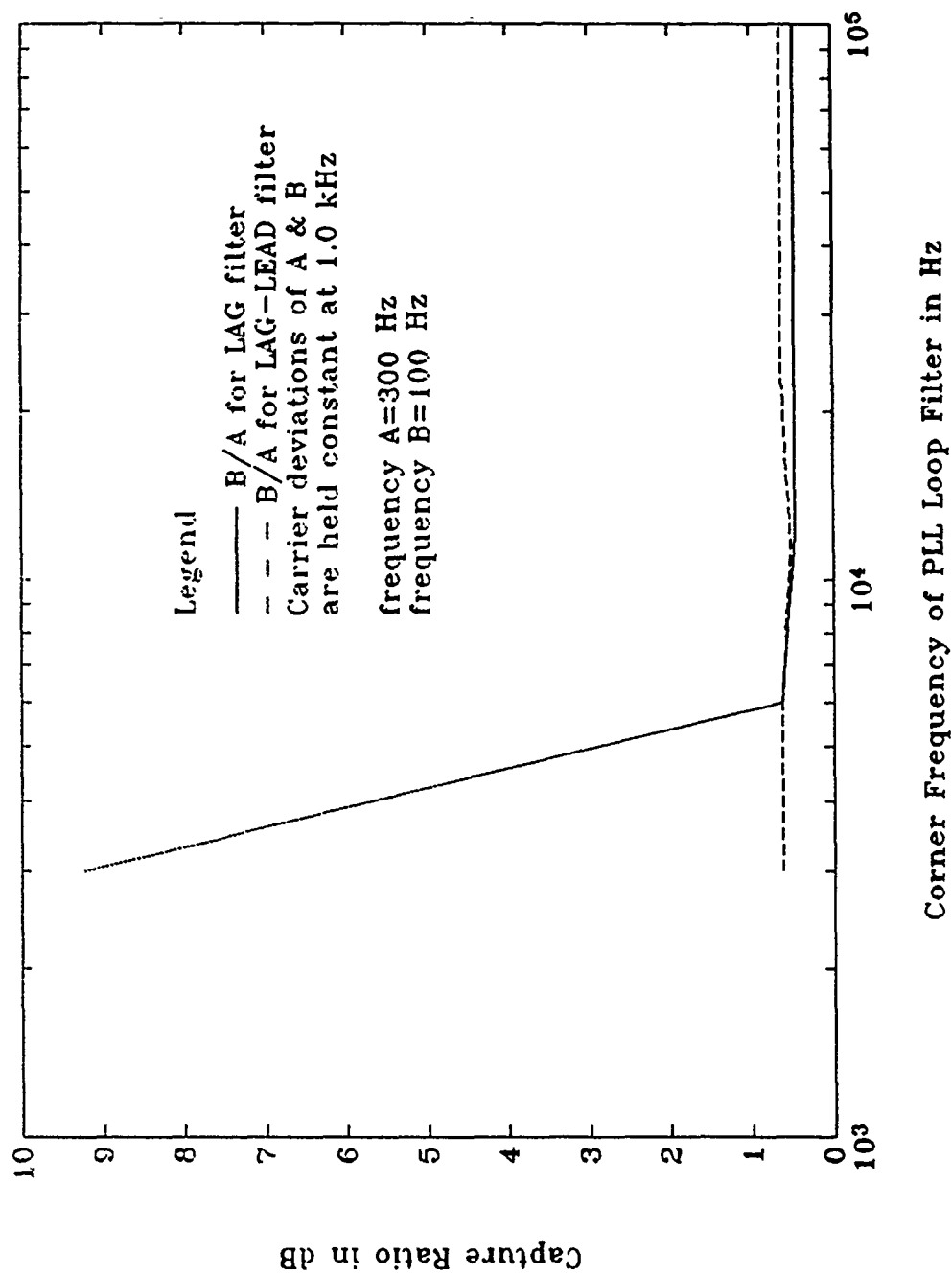


Figure 38. Capture Ratio (A/B) vs. Bandwidth of PLL Loop Filter.

## V. CONCLUSIONS

The experimental system successfully proved the existence of capture effect and permitted an investigation of the effect of various system parameters on capture. The smallest measured value of capture ratio is 0.387 dB. The ease with which system parameters can be changed allowed large amounts of data to be collected quickly.

The frequency deviation of the FM signal is a key parameter when measuring capture ratios. As frequency deviation increases, the capture ratio increases. The frequency deviation of the stronger signal affects capture ratio. The frequency deviation of the weaker signal has no effect on capture ratio.

The frequency of the input message has a small effect on capture ratio. As the frequency of the message increases, the capture ratio increases. This effect is not pronounced.

The PLL loop filter of choice for this system is the lag-lead filter. The lag-lead filter provides smaller values of capture ratio at smaller values of bandwidth. The two filter designs have similar values of capture ratio at larger values of bandwidth.

## APPENDIX A. CIRCUIT SCHEMATICS

This appendix contains the schematic diagrams and a detailed explanation of component values and component selection. Standard analog linear integrated circuits are used. The power supplied to all chips and the breadboard is +14 and -14 volts.

### A. TRANSMITTER.

The transmitter consists of two identical independent channels labeled channel A and channel B. These two channels are shown in Figure 39 on page 55. Since the two channels are identical, a detailed description of only channel A is presented.

The message (message A in) originates from a Wavetek model 145 Pulse/Function generator. The message is frequency modulated by an ICL 8038 precision waveform generator/voltage controlled oscillator (VCO). To have the input message DC-biased to the rest voltage of the VCO, an LM301 operational amplifier (op amp) is used. The op amp is configured as an inverting summer. This op amp sums the input message with a variable voltage that is selected to obtain the chosen VCO rest frequency. The input message amplification can be adjusted at this stage.

The VCO is biased to have a rest frequency of 64.5 kHz. This rest frequency is designed with resistors R5, R6, and R7 and capacitors C2 and C3 using the following relationship:

$$f_R = \frac{.3}{(R5 + R6 + R7)(C2 + C3)} \quad (A.1)$$

For the values chosen and shown in Figure 39, the rest frequency is 50 kHz. A plot of the VCO characteristics identifies the VCO linear region. Note that this value of 50 kHz is for no DC bias on the input message. By DC biasing the input message to a value of approximately 10.5 volts, the VCO will have a rest frequency of 64.5 kHz. The sine wave output of the VCO is taken from pin 2.

The VCO output is applied to an LM318 op amp configured as a noninverting follower with adjustable gain via resistor R12. The follower is used to match impedances between the VCO and the summing amp. The LM318 is chosen for its guaranteed 50V/ $\mu$ sec slew rate. This proved sufficient in amplifying the frequency modulated signal centered at 64 kHz.



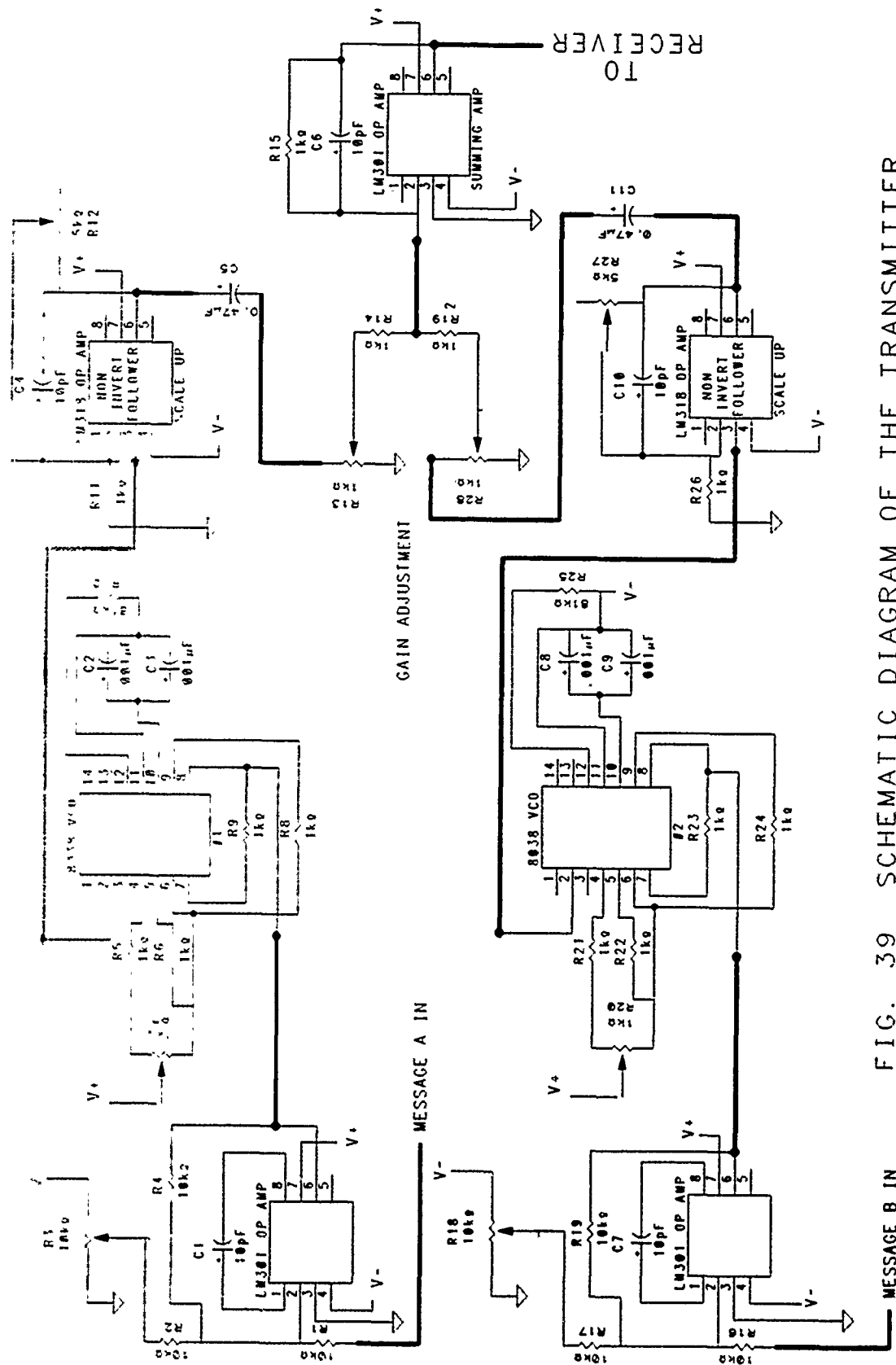


FIG. 39 SCHEMATIC DIAGRAM OF THE TRANSMITTER.

The output of the voltage follower is applied to a potentiometer R13 which allows a further reduction in signal amplitude. The resistors R13 for channel A and R28 for channel B are the primary amplitude adjustments used for the measurement of signal amplitude while observing capture effect.

The signals from channel A and B are combined (summed) in an LM301 op amp configured as an inverting summing amp with no signal gain. The LM301 is also chosen for its large value of slew rate.

## B. RECEIVER.

The signal from the transmitter first encounters an LM318 op amp configured as a voltage follower as shown in Figure 40 on page 57. The follower matches the high output impedance of the summing amplifier in the transmitter to the input of the hard limiter.

The hard limiter is constructed from an LM318 op amp that is configured as an inverting amp with infinite feedback resistance. Resistors R30 and R31 at the output of the follower and hard limiter are used to control the signal amplitude and to prevent distortion.

From the output of the hard limiter, the signal is applied to the LM565 phase-locked loop (PLL). The rest frequency of the PLL is set equal to that of the VCO in the transmitter. The values of surrounding resistors and capacitors determine the PLL rest frequency, capture range, tracking range and loop filter bandwidth.

In the configuration shown, the rest frequency  $f_0$  in Hertz is determined using the following relationship.

$$f_0 = \frac{1.2}{4(R34)(C14)} \quad (A.2)$$

Note that R34 is a potentiometer so that the PLL rest frequency can be fine-tuned to match that of the transmitting VCO. When R34 is adjusted to 2.3 k $\Omega$ , the rest frequency is approximately 64 kHz.

The lock range  $f_L$  is

$$f_L = \frac{8f_0}{V_{cc}} \quad (A.3)$$



FIG. 40 SCHEMATIC DIAGRAM OF THE RECEIVER.

For  $f_0 = 64$  kHz and supply voltage  $V_{cc} = 14$  V, the lock range  $f_L = 36$  kHz. This is a limiting factor in determining the maximum value of carrier frequency deviation  $\Delta f$  which can be applied to the PLL and still maintain capture.

The capture range  $f_{CAP}$  of the PLL is

$$f_{CAP} = \left( \frac{1}{2\pi} \right) \sqrt{\frac{2\pi f_L}{3600(C13)}} \quad (A.4)$$

For the values shown in Figure 40, the capture range  $f_{CAP} = 28.2$  kHz. A capture range of 28.2 kHz limits the frequency deviation of the signal to 14 kHz. The experimental system shows an actual upper limit on capture range of 12 kHz.

The output of the phase detector in the PLL contains sum and difference frequency terms. The loop filters used do not remove all of the sum frequency terms. Therefore, the output of the PLL is applied to an active lowpass filter. Two filters are constructed with different bandwidths. The message frequency determines which filter can be used. Messages with frequencies up to 100 Hz are applied to the 1 kHz filter. All other messages are applied to the 3 kHz filter. The active filters are constructed using LM301 op amps. The corner frequency  $f_{BW}$  of the filter is

$$f_{BW} = \frac{1}{2\pi RC} \quad (A.5)$$

For the 3 kHz bandwidth filter,  $R = R35 = R36$  and  $C = C15 = C17$ . For the 1 kHz bandwidth filter,  $R = R37 = R38$  and  $C = C19 = C20$  as shown in Figure 40. The output of the active filter is the message of the dominant carrier.

## APPENDIX B. PLL LOWPASS FILTER DESIGN.

The LM565 phase-locked loop allows for two separate designs of the loop lowpass filter. These are the simple lag filter and the lag-lead filter. The IC chip has an internal 3.6 k $\Omega$  resistor in series with an external connection to which one of the above two filters can be attached. Figure 41 on page 60 is a diagram of both of these filters and how they are connected to the PLL chip. The gains of the phase detector and VCO internal to the PLL affect the bandwidth of the loop filter. From [Ref 5] gains are combined into a term  $K_0K_D$ . This gain term is calculated using the following formula

$$K_0K_D = \frac{33.6(f_{0C})}{V_{cc}} \quad (B.1)$$

where  $f_{0C}$  is the PLL center frequency and  $V_{cc} = 14$  Volts. Using the above equation, the value for  $K_0K_D$  is 154,800. For the simple lag filter seen in Figure 41, the corner frequency  $f_n$  of the filter is

$$f_n = \frac{1}{2\pi} \sqrt{\frac{K_0K_D}{(R1)(C1)}} \quad (B.2)$$

The value of resistor R1 is 3.6 k $\Omega$  and capacitor C1 is chosen to fit the desired bandwidth. Rearranging the above equation gives

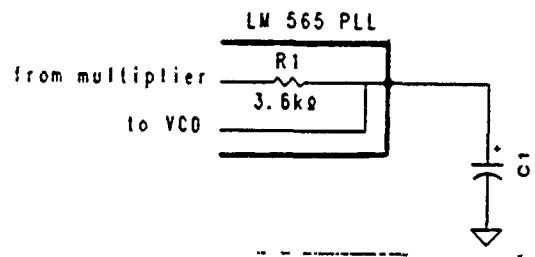
$$C1 = \left( \frac{1.043}{f_n} \right)^2 \quad (B.3)$$

The filter damping factor  $\delta$  is determined for the lag filter by using the following equation

$$\delta = \frac{1}{2} \sqrt{\frac{1}{R1(C1)K_0K_D}} \quad (B.4)$$

The desired value of  $\delta$  is between 0.5 and 1.0. Using the above relationships, the lag filter can be designed.

### Lag Filter



### Lag Lead Filter

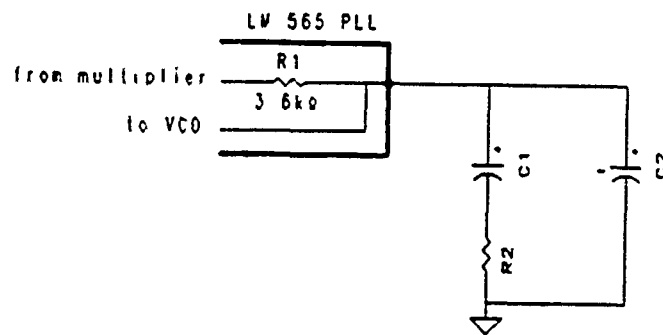


Figure 41. PLL Filter Designs.

The lag-lead filter shown in Figure 41 has different equations for filter bandwidth and damping factor. The equation for the corner frequency is

$$f_n = \frac{1}{2\pi} \sqrt{\frac{K_0 K_D}{\tau_1 \tau_2}} \quad (B.5)$$

where  $\tau_1 = (R1)(C1)$  and  $\tau_2 = (R2)(C1)$ . The value of  $C2$  is chosen such that  $C2$  is less than 10% of  $C1$ . The damping factor  $\delta$  is computed from

$$\delta = \pi f_n(\tau_2) = \pi f_n(R2)(C1) \quad (B.6)$$

The damping factor is desired to be about 0.75.

The method of filter design for the lag lead filter is as follows. A corner frequency and a value of  $\delta$  are chosen. From the equation for corner frequency,

$$\tau_1 + \tau_2 = \left( \frac{K_0 K_D}{(2\pi f_n)^2} \right) \quad (B.7)$$

It is also known that

$$\tau_1 + \tau_2 = (R1 + R2)C1 \quad (B.8)$$

With  $R1$  fixed at 3.6 k $\Omega$  and using

$$C1 = \frac{\delta}{\pi f_n(R2)} \quad (B.9)$$

there are two equations with two unknowns  $R2$  and  $C1$ . Once  $R2$  is determined, the value of  $C1$  is found.

To demonstrate the frequency response of both of these filters, the values of  $R2$ ,  $C1$  and  $C2$  for each filter at a bandwidth of 3 kHz are chosen. Actual data is taken for these filters constructed from resistor/capacitor components external to the PLL. The corner frequency of the filter is not 3 kHz but 350 Hz since the gains of the VCO and phase detector in the PLL are not included. The curves are plotted in Figure 42 on page 63. The values of  $C1$  for the lag filter used in the PLL design is 0.122  $\mu F$ . The value of  $C1$  and  $R2$  in the lag lead design are 0.1  $\mu F$  and 790  $\Omega$ . The value of  $C2$  is 3 pF.

The plot in Figure 42 on page 63 shows that the frequency response of the lag-lead filter is flatter in the pass band and starts to drop off at a larger frequency when compared with the lag filter of the same bandwidth.



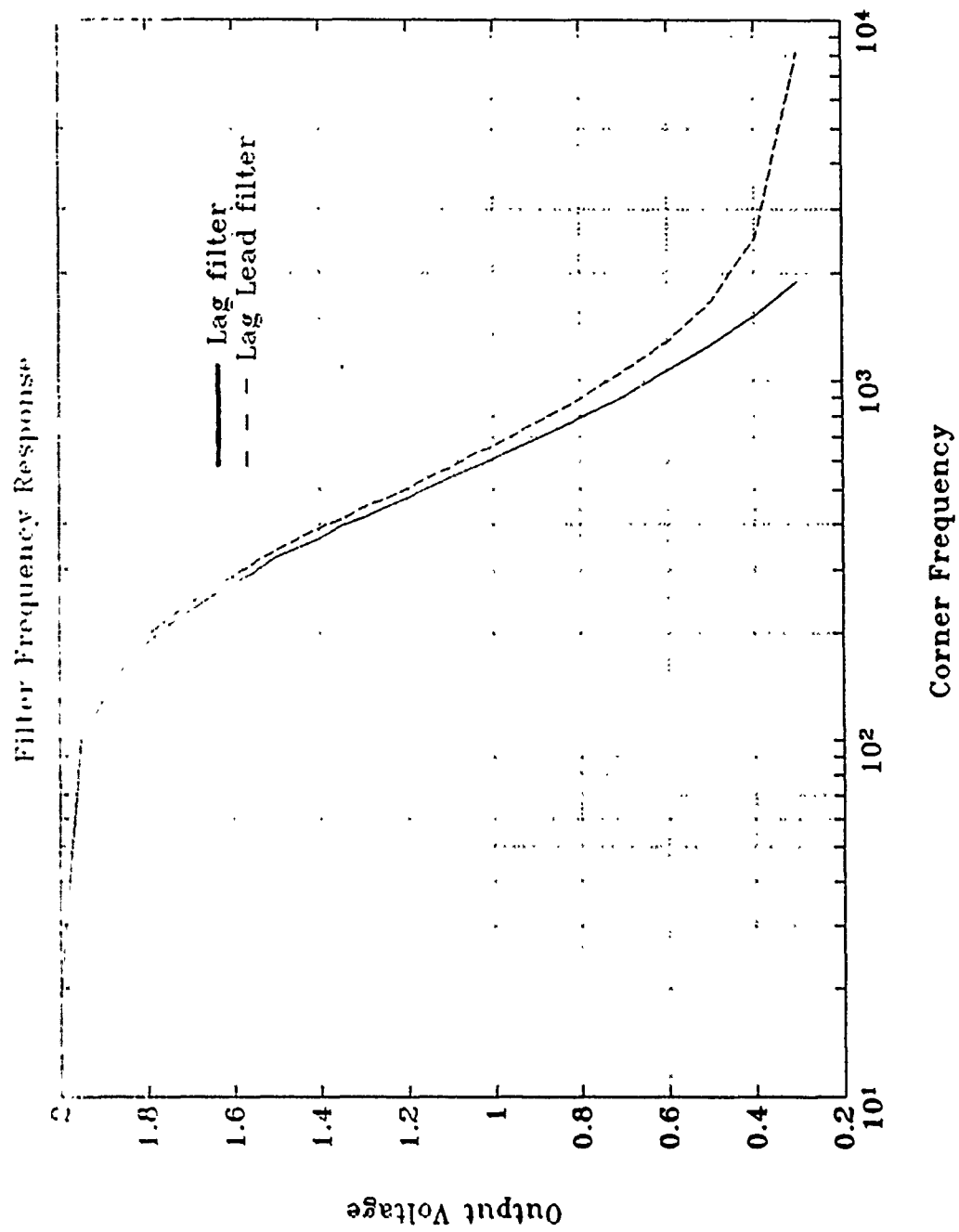


Figure 42. Frequency Response of the PLL Loop Filters.

## LIST OF REFERENCES

1. Haykin, S., *Communication System*, John Wiley and Sons, Inc., 1983.
2. Park, S. S., *On Capture Effect of FM Demodulators*, M.S. Thesis, Naval Postgraduate School, Monterey, California, March 1989.
3. Taub H., and Schilling D. L., *Principles of Communication Systems*, McGraw-Hill Book Co., 1986.
4. Bruyland, I., "The Influence of Finite Bandwidth on the Capture Effect in FM Demodulators", *IEEE Transactions on Communications*, Vol. COM-26, No. 6, pp. 776-784, June 1978.
5. National Semiconductor, *Linear Databook*, 1989.

## INITIAL DISTRIBUTION LIST

	No. Copies
1. Defense Technical Information Center Cameron Station Alexandria, VA 22304-6145	2
2. Library, Code 0142 Naval Postgraduate School Monterey, CA 93943-5002	2
3. Department Chairman, Code 62 Department of Electrical Engineering Naval Postgraduate School Monterey, CA 93940	1
4. Professor G.A. Myers, Code 62Mv Department of Electrical Engineering Naval Postgraduate School Monterey, CA 93940	5
5. Professor T. T. Ha, Code 62Ha Department of Electrical Engineering Naval Postgraduate School Monterey, CA 93940	1
6. LT. D.G. Bevington 10927 Battersea Lane Columbia, MD 21044	2
7. P. Evans Naval Air Test Center Mail Code SY81 Patuxent River, MD 20670	1